Quaternary Research (2024), 1–18
doi:10.1017/qua.2023.69

Research Article

Implications of the geochemistry of L1LL1 (MIS2) loess in Poland for paleoenvironment and new normalizing values for loess-focused multi-elemental analyses

Jacek Skurzyński[a], Zdzisław Jary[a], Kaja Fenn[b], Frank Lehmkuhl[c], Jerzy Raczyk[a], Thomas Stevens[d] and Małgorzata Wieczorek[a]

[a]Institute of Geography and Regional Development, University of Wrocław, 1 Uniwersytecki Sqr., 50-137 Wrocław, Poland; [b]Department of Geography and Planning, University of Liverpool, Liverpool L69 7ZT, UK; [c]Department of Geography, Wüllnerstr. 5b, RWTH Aachen University, 52062 Aachen, Germany and [d]Department of Earth Sciences, Uppsala University, Villavägen 16, Uppsala, 75236, Sweden

Abstract

Loess paleoenvironmental reconstructions on regional to supra-regional scales have recently gained much attention. Geochemistry comparisons in relation to reference datasets, such as the Upper Continental Crust (UCC) data, have furthered our understanding of the climatic and geomorphological conditions under which terrestrial sites have developed. However, UCC data differs from loess, thereby obscuring important features, and the existing "average loess" datasets also are not sufficient for modern investigations.

In this study, we examine the youngest Polish loess (L1LL1 = MIS 2, ca. 26–15 ka) for its suitability as a new, loess-focused reference dataset. Eighty-nine samples from seven sites were analyzed, using inductively coupled plasma spectrometry. The loess had assumedly been homogenized during transportation and/or sedimentary recycling (La_N/Sm_N = 3.34–4.06, median 3.78; Eu/Eu^* = 0.46–0.66, median 0.55; Gd_N/Yb_N = 1.08–1.49, median 1.26), and weakly affected by pre- or post-depositional weathering (CIA = 53.64–69.12, median 57.69). The statistically significant differences between sites in elemental medians were mostly conditioned by variations in grain size and in the "fresh" to "re-deposited" sediment ratio. Nonetheless, the overall geochemical composition homogeneity provided a basis for the estimation of Polish Median Loess (PML) data, as determined for 41 chemical elements. When used, PML data highlight differences between loess regions in Europe, thereby providing a tool for cross-continental comparisons.

Keywords: Elemental composition, Inductively coupled plasma, Late Pleistocene, Aeolian, Central Europe, PML, Polish median loess

INTRODUCTION

Loess is a clastic mineral dust deposit that occurs as wind-laid sheets (Smalley and Vita-Finzi, 1968) and is considered as one of the most investigated and best recognized terrestrial sediments (Schaetzl et al., 2018; Waroszewski et al., 2021). Its bulk properties (such as granulometric or mineralogical composition) show important variations with age, location, source area, topography, or depositional and post-depositional weathering history (Lehmkuhl et al., 2016, 2021; Rousseau et al., 2018; Pötter et al., 2023). At the same time, loess is considered to be relatively homogeneous in terms of geochemical composition (Gallet et al., 1998; Wright et al., 1998; Tripathi and Rajamani, 1999; Újvári et al., 2008; Muhs, 2018; Fenn et al., 2022) due to its considerable spread and mixing during transport. Consequently, its chemical composition was initially used mainly for stratigraphic locations of the boundaries of individual layers (Sial et al., 2019), based on the assumption that soil processes lead to the re-deposition of mobile and retention of immobile elements (Buggle et al., 2011).

Contemporary chemostratigraphic studies of loess have focused on specific causes of stratigraphic and spatial variation in chemical composition (Sial et al., 2019). However, they are limited by the lack of representative sets of geochemical data from potential source areas (Buggle et al., 2008; Újvári et al., 2008). Some authors have compared the chemical composition of loess with floodplain sediments (Muhs and Budahn, 2006; Buggle et al., 2008; Újvári et al., 2014; Skurzyński et al., 2020), which represent the average composition of large areas and have been suggested as an immediate, up-wind source of silty material (Smalley and Leach, 1978; Hao et al., 2010; Schaetzl and Attig, 2013; Stevens et al., 2013; Obreht et al., 2015; Fenn et al., 2022; Költringer et al., 2022). Other studies have compared the chemical signatures between loess–paleosol stratigraphic sequences (e.g., Buggle et al., 2008; Újvári et al., 2008; Skurzyński et al., 2019; Pötter et al., 2021). However, this approach may present different challenges due to the methodological differences of determining the chemical composition (e.g., Miyazaki et al., 2016; Pötter et al., 2021), which may result in significantly different values

Corresponding author: Jacek Skurzyński; Email: jacek.skurzynski@uwr.edu.pl

Cite this article: Skurzyński J, Jary Z, Fenn K, Lehmkuhl F, Raczyk J, Stevens T, Wieczorek M (2024). Implications of the geochemistry of L1LL1 (MIS2) loess in Poland for paleoenvironment and new normalizing values for loess-focused multi-elemental analyses. *Quaternary Research* 1–18. https://doi.org/10.1017/qua.2023.69

for the various chemical elements (Skurzyński and Fenn, 2022). One of the most common comparative approaches is the use of normalized multi-element diagrams (e.g., Gallet et al., 1998; Jahn et al., 2001; Buggle et al., 2008; Újvári et al., 2008, 2014; Rousseau et al., 2014; Campodonico et al., 2019; Bosq et al., 2020; Skurzyński et al., 2020). These so-called spider diagrams (or spidergrams) are constructed with respect to reference datasets such as the average composition of the upper continental crust (UCC) (Taylor and McLennan, 1985; Condie, 1993; McLennan, 2001; Rudnick and Gao, 2003) or post-Archaean Australian average shale (PAAS) (Taylor and McLennan, 1985), and identify deviations in composition from the reference dataset (Rollinson, 2013). However, data reporting is poor, with some studies not providing information on source of the normalization dataset (e.g., the version of the UCC).

Crucially, because the chemical composition of loess differs significantly from the UCC or PAAS, it results in strong positive or negative anomalies (e.g., Skurzyński et al., 2020), which obscures other changes between individual samples. Consequently, attempts have been made to create a set of normalizing values dedicated to loess, such as the average loess (Schnetger, 1992; presented later in a limited form as AVL^1 by Újvári et al., 2008) or global average loess (GAL; Újvári et al., 2008). AVL^1 was calculated using 24 samples taken from seven loess regions (Lukashev et al., 1965; Ebens and Connor, 1980; Taylor et al., 1983), and GAL was based on the mean of 17 averages from 11 loess regions (244 samples, including these used for AVL^1), with different quality of age control, and analyzed by different or even unreported methods (Lukashev et al., 1965). Although GAL data constitute a significant contribution to the understanding of loess geochemistry, they present data for only a limited number of chemical elements (even in relation to the original average loess by Schnetger, 1992) and lack most of the trace elements and rare earth elements (REE), which are particularly important from a perspective of provenance studies because major elements do not distinguish source contributions (e.g., Skurzyński et al., 2020; Fenn and Prud'homme, 2022). Consequently, both GAL and other existing 'average chemical loess compositional data' are not sufficient for the comparative analysis of loess from different parts of Europe or the world, and alternative reference data sets (such as UCC) are not suited to the needs of loess research. Therefore, the old general assumption is valid – there is a need to introduce a set of consistent and universally accepted normalizing values (Rock, 1987; Rollinson, 2013).

This study tackles this dilemma by presenting a new dataset dedicated to loess, based on samples representing weakly weathered and relatively homogenous loess from areas with well-documented chronostratigraphy, and measured with similar, reliable and precise methods. The loess cover of Poland was chosen for this initial analysis because it is thought to represent the entire Northern European Loess Belt. It reflects contemporary and Pleistocene features of European climate: continental in the east and more oceanic in the west (Cegła, 1972; Jersak, 1973; Maruszczak, 1991; Jary, 2007; Jary and Ciszek, 2013). It also is lithologically diverse in relation to the latitudinal extent of the Pleistocene extra-glacial zone (Tutkovsky, 1899; Jahn, 1950). Consequently, we argue that the loess of eastern Poland shares many similarities (e.g., in the granulometric composition) with the East European loess cover, while the western part is similar to the western loess deposits (Maruszczak, 1991). Moreover, the last glacial maximum (LGM) loess in Poland (L1LL1 correlated to MIS 2, ca. 26–15 ka) was demonstrated to have been strongly homogenized during transportation and/or sedimentary recycling, and has not been significantly affected by pre- or post-depositional processes (Skurzyński et al., 2020). Thus, we analyzed 89 loess samples from seven research sites, for major, trace, and rare earth element concentrations to determine the factors influencing the chemical compositions of Polish loess, and to propose new reference values of loess geochemical composition.

RESEARCH AREA AND MATERIALS

The loess cover of Poland relates to the very dynamic environment of Pleistocene glaciations (e.g., Tutkovsky, 1899; Jahn, 1950; Rousseau et al., 2014; Skurzyński et al., 2020) and was most likely sourced from glaciogenic deposits that were homogenized by meltwater rivers (Smalley et al., 2009, Badura et al., 2013; Pańczyk et al., 2020; Baykal et al., 2021), with a variable proportion of local material (Pańczyk et al., 2020, Baykal et al., 2021). Loess sites selected for sampling represent the full variability of the loess in Poland (Fig. 1). The sites were divided into main and supplementary ones, considering the scope of geochemical analyses and the accuracy of age control. We used the 'universal' stratigraphical labeling system, first introduced by Kukla and An (1989) and modified by Marković et al. (2008, 2015), for this loess.

The L1LL1 loess units were sampled at these sites: Biały Kościół (Moska et al., 2019a), Złota (Moska et al., 2018; Skurzyński et al., 2020), and Tyszowce (Moska et al., 2017; Skurzyński et al., 2019). These sites have existing chronologies developed using optically stimulated luminescence (OSL) dating (Fig. 2), and they have been analyzed at high resolution for geochemistry. The main sites (representing the variability of loess on the W–E axis, located at considerable distances from each other, and near the valleys of various large rivers) represent the domain of the Northern European Loess Belt (domain II; Lehmkuhl et al., 2021), but each likely formed under different paleoenvironmental conditions (e.g., Maruszczak 1991). Biały Kościół belongs to subdomain IIb (Western European continental subdomain), and the rest of the sections belong to subdomain IIc (Central European continental subdomain) (Lehmkuhl et al., 2021). All of these loess sequences were formed during the last interglacial–glacial (Fig. 2), although there are notable differences in the thickness of individual loess covers (Fig. 2), which indicates different depositional rates. This further implies local influences on the development of each profile on a sub-orbital scale, as suggested by Fenn et al. (2021).

The lithological features of the main research sites are also varied (Fig. 2). In the L1LL1 section at Biały Kościół (especially in the lower part), weak tundra-gley soils, which indicate periglacial deformation, or horizons of initial gleying can be distinguished (Moska et al., 2019a). At Złota, the L1LL1 loess is more homogeneous, although several horizons of initial gleying and/or deformation are also present (Fig. 2). The lowest parts are deformed by cryogenic processes and show traces of slope redeposition (Moska et al., 2018; Skurzyński et al., 2020). At Tyszowce, where the L1LL1 loess can be as much as 14 m thick (Fig. 2), sandy laminae are common in the upper part (to a depth of ~5 m below ground level) (Fig. 2), suggesting short-term episodes of material transport from the nearby Huczwa River valley (Skurzyński et al., 2019). Two generations of ice wedge pseudomorphs in the L1LL1 loess indicate a double development cycle and degradation of permafrost (Jary, 2007).

https://doi.org/10.1017/qua.2023.69 Published online by Cambridge University Press

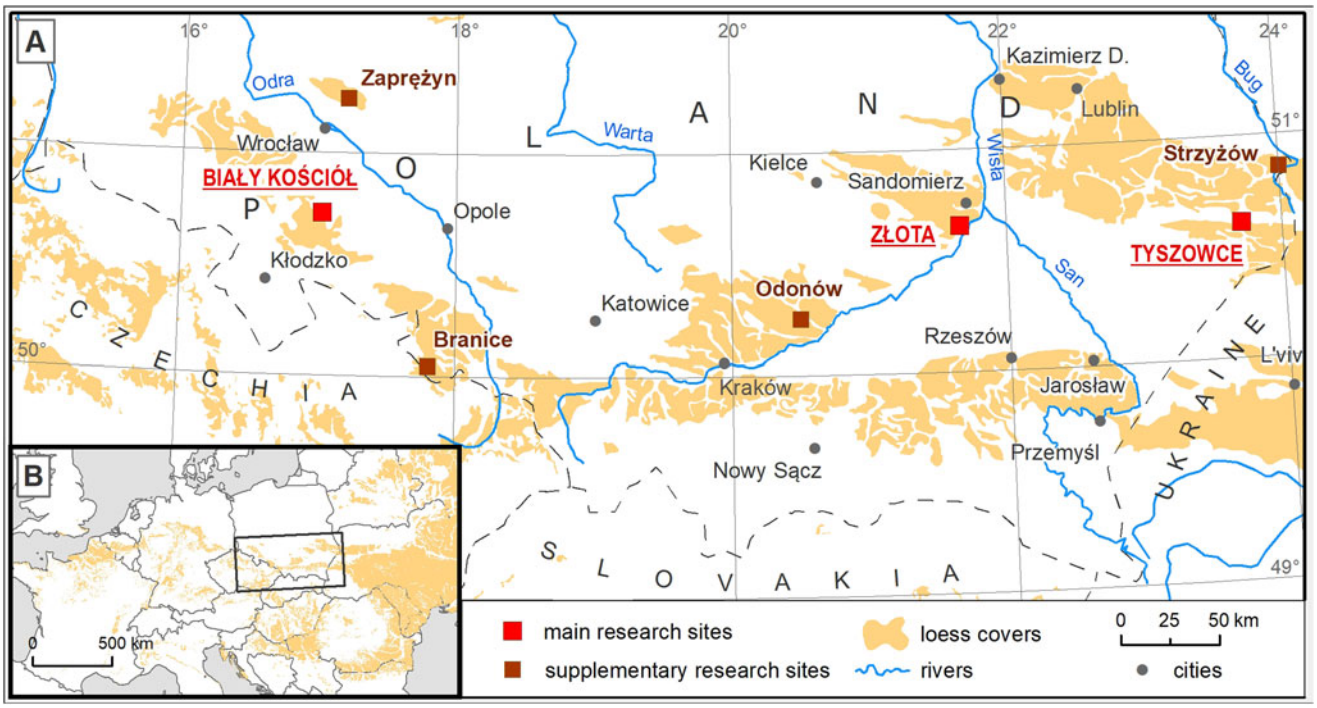

Figure 1. (A) Location of the research sites on a map of loess distribution in Poland and (B) Europe. Loess distribution after Lehmkuhl et al. (2021).

Four supplementary sites—Zaprężyn (Jary, 2007; Krawczyk et al., 2017; Skurzyński et al., 2017; Zöller et al., 2022), Strzyżów (Moska et al., 2019b), Branice (Jary, 2007; Moska and Bluszcz, 2013) and Odonów (Butrym, 1987; Jary, 2007)—also were investigated to determine the spatial variability of the chemical composition in the context of hetero- or homogeneity of the source material. The sites at Zaprężyn and Strzyżów are located farther north than Biały Kościół, Złota, and Tyszowce, and the sections at Branice and Odonów represent the southern parts of the loess in Poland (Fig. 1).

In this work, 70 L1LL1 (MIS 2) samples were subjected to geochemical analysis (Biały Kościół, 19; Tyszowce, 32; Zaprężyn, 3; Strzyżów, 6; Odonów, 5; Branice, 5) following the methodology used previously for the Złota loess–paleosol sequence (Skurzyński et al., 2020). Nineteen additional published samples for Złota's (Skurzyński et al., 2020) L1LL1 loess also were included, resulting in a total of 89 L1LL1 (MIS 2) loess samples that were studied.

METHODS

The loess samples were collected in 2012 (Tyszowce, Złota, and Zaprężyn), 2013 (Strzyżów), and 2018 (Biały Kościół). Samples from two of the sites (Branice and Odonów) are the result of earlier works (2002), although the methodology used at that time did not significantly differ from that developed for the new research sites (Jary, 2007). The air-dried samples were stored in plastic string bags.

Chemical analyses were performed in a commercial laboratory (Bureau Veritas, formerly ACME labs; LF200 package) using inductively coupled plasma – emission spectrometry (ICP–ES) and inductively coupled plasma – mass spectrometry (ICP–MS) after sample fusion with lithium borate (in a furnace) and a cooled alloy dissolution with American Chemical Society-grade nitric acid. Prior to the analysis, the material was passed through a 63-µm dry sieve to avoid the effect of grain-size differentiation on geochemical parameter values (e.g., Nesbitt and Young, 1982; Shao et al., 2012; Guan et al., 2016) and to minimalize the influence of very local sandy material (Skurzyński et al., 2019).

Analytical precision relative standard deviation (RSD) data were estimated separately for each of the measurement series, based on several measurements (Table S1) of the certified STD SO-19 standard (internal Bureau Veritas standard, unpublished). The average values for a given element were close to the expected value of the share of the analogous element in the STD SO-19 standard, and the differences between the average values from individual series were usually negligible (Table S1). The RSD is less than ± 5% for most of the elements determined, and the variation between measurement series is usually small (Table S1). For Cs, Ga, Hf, and W, in some measurement series, the RSD was less than ± 10%. For Be (which is not significant in the context of this paper), the RSD was more variable, ranging from ± 4.79% to ± 34.41% in individual measurement series (Table S1).

The grain sizes of the samples were determined by a Malvern Mastersizer 2000 laser grain-size analyzer, which has a measurement range of 0.02–2000 µm with a precision of ± 1%. The refractive and absorption indices used in the measurements were 1.544 and 0.1, respectively. Measurements were conducted after chemical pre-treatment. The samples were first treated with H_2O_2 and 10% HCl to remove organic matter and carbonate, respectively. Finally, the samples were dispersed with a 0.5 N sodium metaphosphate solution and ultrasonicated for 10 min before measuring (e.g., Song et al., 2014; Skurzyński et al., 2019). The clay–silt boundary assigned to the samples was 4 µm (e.g., Svensson et al., 2022), so the clay fraction may be underestimated in relation to data from publications utilizing a higher clay–silt boundary (e.g., 8 µm; Konert and Vandenberghe, 1997).

https://doi.org/10.1017/qua.2023.69 Published online by Cambridge University Press

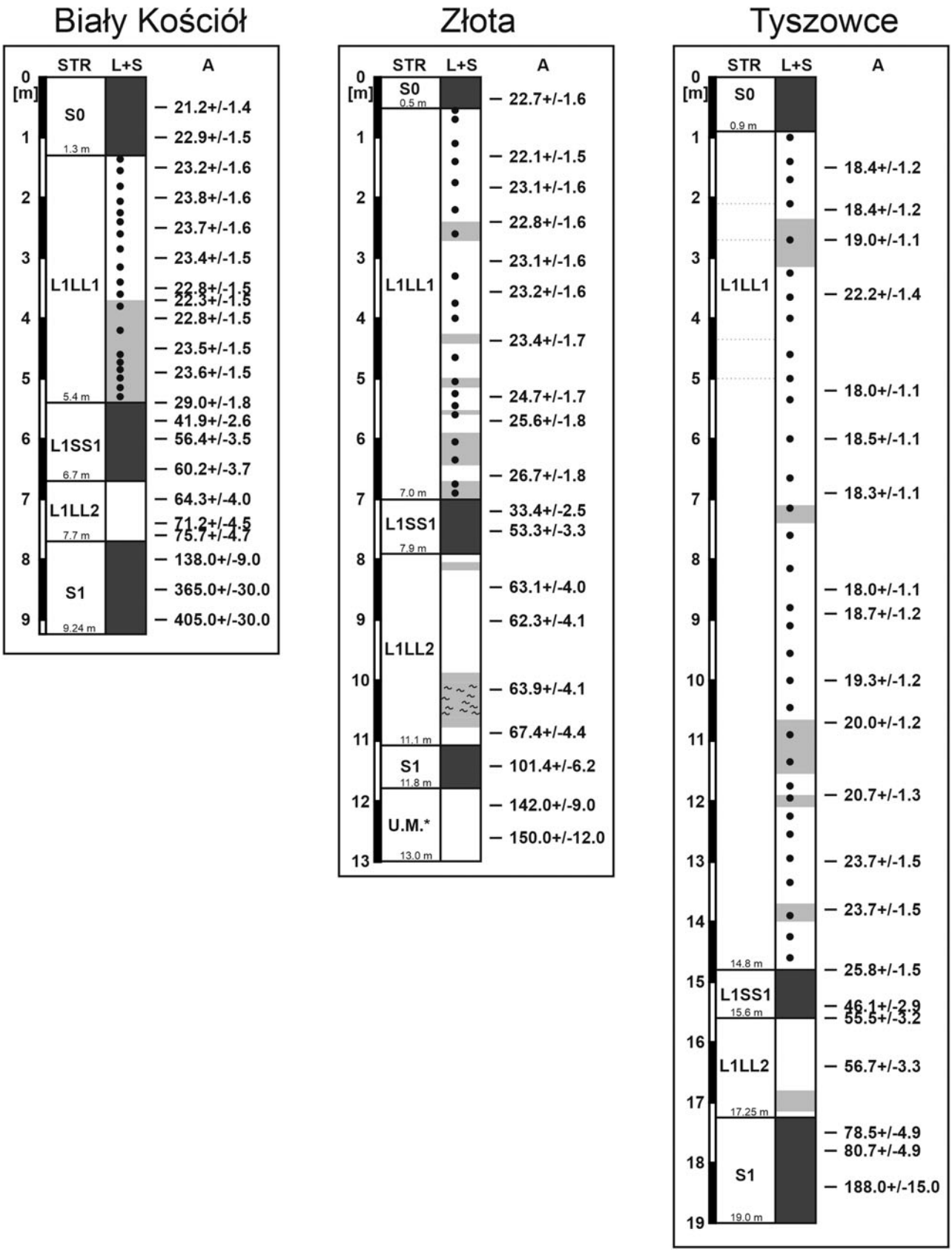

Figure 2. Schemes of the main research sites. Abbreviations: STR = stratigraphy; L+S = lithology + samples; A = ages (expressed as ka); S0 = recent soil; L1LL1 = loess correlated to MIS 2; L1SS1 = paleosol correlated to MIS 3; L1LL2 = loess correlated to MIS 4; S1 = paleosol complex correlated to MIS 5; U.M.* = underlying material. Stratigraphical labeling system after Kukla and An (1989), modified by Marković et al. (2008, 2015). Dark gray rectangles = soil units; pale gray rectangles = horizons with signs of gley processes or deformation; pale grey rectangle with black squiggles = loess with gley and humic intercalations; black spots = geochemical samples. Ages after Moska et al. (2017, 2018, 2019a) – Post-IR IRSL polymineral fraction (4–11 μm).

https://doi.org/10.1017/qua.2023.69 Published online by Cambridge University Press

The concentrations of major (wt. %), trace, and rare earth (ppm) elements, as well as values of geochemical parameters and granulometry, are shown in Table S2. Basic, descriptive statistics (median, average, minimum, maximum, and standard deviation) are presented in Table S3. Throughout this article, the median (instead of the mean) is used because most proportions of chemical elements (except Na_2O, K_2O, TiO_2, Ba, Sr, Y, and almost all of the REEs) are not normally distributed (tested using the Shapiro–Wilk test; Table S4). Consequently, the non-parametric Kruskal–Wallis one-way analysis of variance (Kruskal–Wallis test; Table S4) and Spearman's rank correlation coefficient were used for most analyses. The number of samples from supplementary sites was too limited for statistical analysis, therefore comparison of the whole dataset was performed using the geochemical diagrams.

RESULTS

Chemical composition and granulometric background of the main research sites

The Kruskal–Wallis test (Table S4), in which the null hypothesis is that the medians of each group are the same, showed that at least at one main research site the loess chemical composition differs significantly from the others, by the median of practically all of the determined chemical elements (except MgO, P_2O_5, MnO, Ni, and Zr).

Biały Kościół, as compared to the rest of main sites, is characterized by the highest median values for most chemical elements (except SiO_2, CaO, and Sr), and the highest minimum values for many major-element oxides (Al_2O_3, Fe_2O_3, K_2O, TiO_2, MnO) and all trace and rare earth elements (except Hf, Sr, and Zr). The maximum values from Biały Kościół also are the highest in the entire dataset scale for most oxides (Al_2O_3, Fe_2O_3, MgO, K_2O, and TiO_2) and trace elements (except Co, Ga, Hf, Nb, Sr, V, W, and Zr), and for all REEs (Table S3). In addition, it is the only profile where Ni was found in most of the samples (Table S2). This site is characterized by the highest minimum values and the highest median of fine fractions (< 4 μm, 4–8 μm, and 8–16 μm), with the lowest median of medium (16–31 μm) and coarse (31–63 μm) silt. The median of sand (> 63 μm) also is the highest, but the maximum value is the lowest in relation to the rest of the main research sites (Table S3). The lower part (from a depth of ~4 m below ground level) is clearly enriched in fine fractions (Table S2).

Złota is poorer in trace elements and REEs than Biały Kościół, and richer in both than Tyszowce (Table S3). However, the highest median of SiO_2, Cr, and W (the latter two equal with Biały Kościół) were found in this profile, as well as the highest minimum values of SiO_2, MgO, Na_2O, P_2O_5, Hf, W, and Zr (Table S3). In terms of grain size, Złota is characterized by the lowest median of fine fractions, and the only significant increase of fine-grained material was found in the lowest part of the L1LL1 loess, just above the L1SS1 soil (Fig. S1). The median and minimum values of medium- and coarse-grained silt were the highest (Table S3). No significant enrichment in the sand fraction was found (Fig. S1).

Loess at the Tyszowce site is the most depleted in the chemical components (if one considers median values), with the exception of CaO and Sr, which reached the highest median values. However, the highest maximum values of SiO_2, CaO, P_2O_5, MnO, Hf, Sr, Ta, W, Zr, and Lu relative to the rest of main research sites were found at Tyszowce (Table S3). Notably all the minimum values at Tyszowce (and the lowest minimum values of the whole dataset) are in the upper, ~5-m thick, sandy part of loess L1LL1 (Table S2). At Tyszowce, the grain-size variation is greater than in the other main sites (Fig. S1, Table S2). For example, the median share of the sand fraction is the lowest (8.73%), with the lowest minimum value (2.09%) and the highest maximum value (40.35%); the standard deviation exceeds 9 (Table S3). Apart from the sand fraction, there is more coarse-grained silt at Tyszowce than at Biały Kościół, but less than at Złota. The share of fine fractions is higher than at Złota, but lower than at Biały Kościół (Table S3). The fine material generally shows a clear upward trend with depth, reaching maximum values in the lower part of the L1LL1 unit, but in several places this trend is disturbed (Fig. S1).

Chemical composition and granulometric background of the supplementary research sites

Due to the limited number of samples from the supplementary sites, Shepard's (1954) triangular diagram, based on Wentworth's (1922) classification, was used to interpret grain sizes (Fig. S2). The use of laser diffraction data could have caused underestimation of the clay fraction (e.g., Konert and Vandenberghe, 1997; Miller and Schaetzl, 2012; Bitelli et al., 2019), however it clearly shows the overall diversity. The loess at Zaprężyn is enriched in the sand fraction in relation to the other supplementary research sites (Fig. S2, Table S2). Loess from Odonów and Strzyżów show more 'pure silt' granulometric characteristics (Fig. S2). Loess at Strzyżów is not as variable in terms of grain size, although the samples represent the part of L1LL1 loess of considerable thickness, from 3.20–9.30 m below ground level. (Table S2). The loess at Branice is distinguished by a significant amount of fine (< 4 μm) fractions (Fig. S2, Table S2), with a low share of coarse-grained silt (31–63 μm) and sand (Table S2). The share of medium-grained silt (16–31 μm) is comparable to other supplementary sites (Tables S2 and S3). The results of the chemical composition of the supplementary research sites, summarized in Table S2 and S3, will be discussed later, to avoid unnecessary repetitions.

DISCUSSION

Stratigraphic variability of the main research sites' chemical compositions

All profiles show minor fluctuations and clear peaks of mobile (e.g., MgO, CaO, or Fe_2O_3; Kabata-Pendias and Pendias, 1999) and immobile (e.g., Zr, Hf, or Nb; Sheldon and Tabor, 2009) oxides and elements (Figs. 3–5; Table S2). This variation could be related to the changes in the mineralogical and/or grain-size composition (e.g., at 11.95-m depth of the Tyszowce profile, where the sharp decrease in REE content was found; Fig. 5). This transition was followed by peaks of Hf, Zr, U, and W (Fig. 4), which may be explained by additions different from the main mass of sediment (as suggested by the strong increase in coarse-grained silt; Fig. S1) from local sources or from sediments enriched in resistant mineral phases.

The variability in chemical composition may be related to post-depositional processes, such as bioturbation, gleying, and weak weathering (e.g., Kemp, 2001; Jeong et al., 2008; Mroczek, 2013). However, no clear influence of the initial tundra-gley

https://doi.org/10.1017/qua.2023.69 Published online by Cambridge University Press

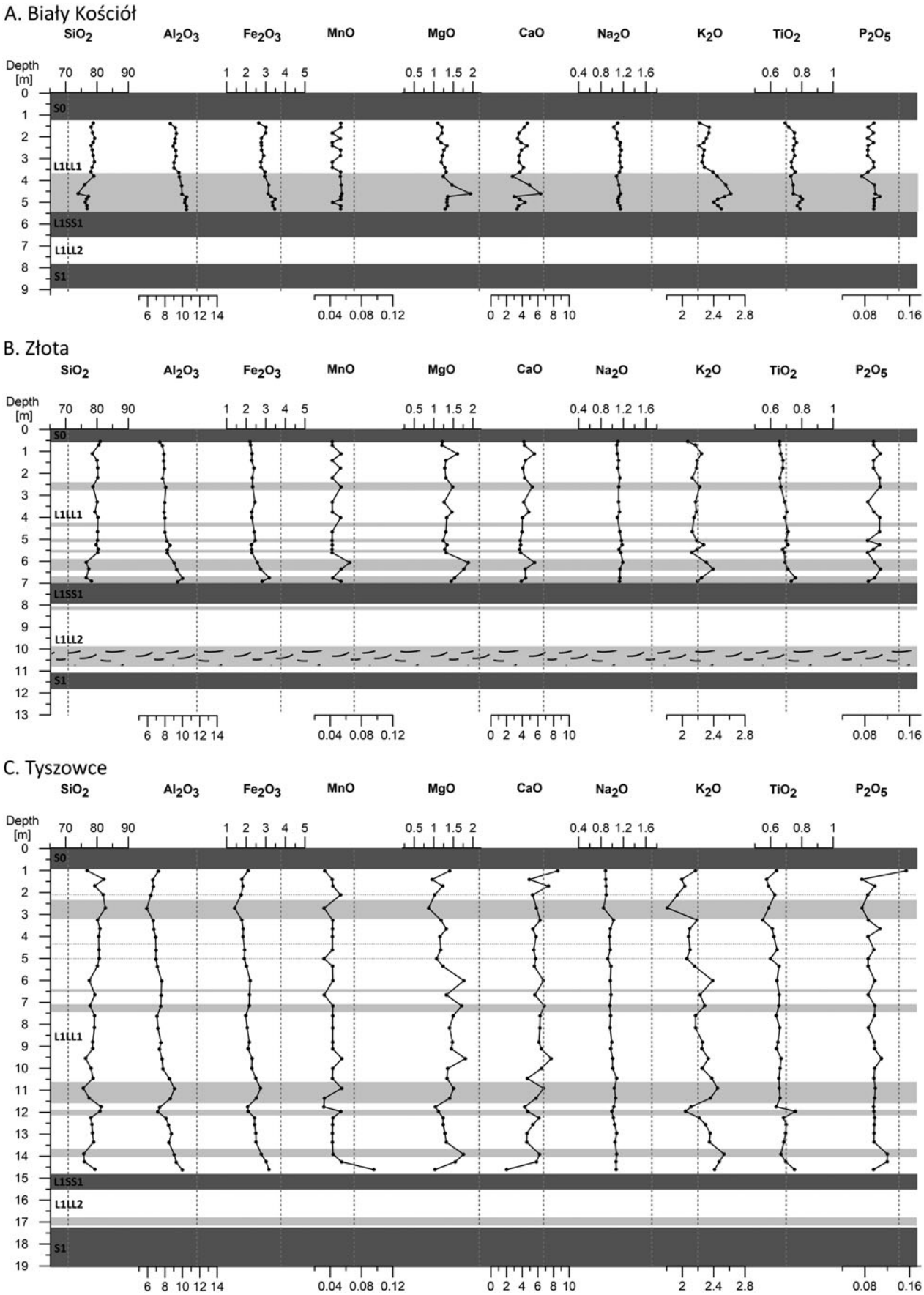

Figure 3. The variability of the main elements (100 wt. % without the volatile components) at the research sites. Vertical gray dashed lines represent GAL values (Újvári et al., 2008) for individual oxides. The main pedo- and lithostratigraphic units are also indicated. See Figure 2 for lithologic legend.

https://doi.org/10.1017/qua.2023.69 Published online by Cambridge University Press

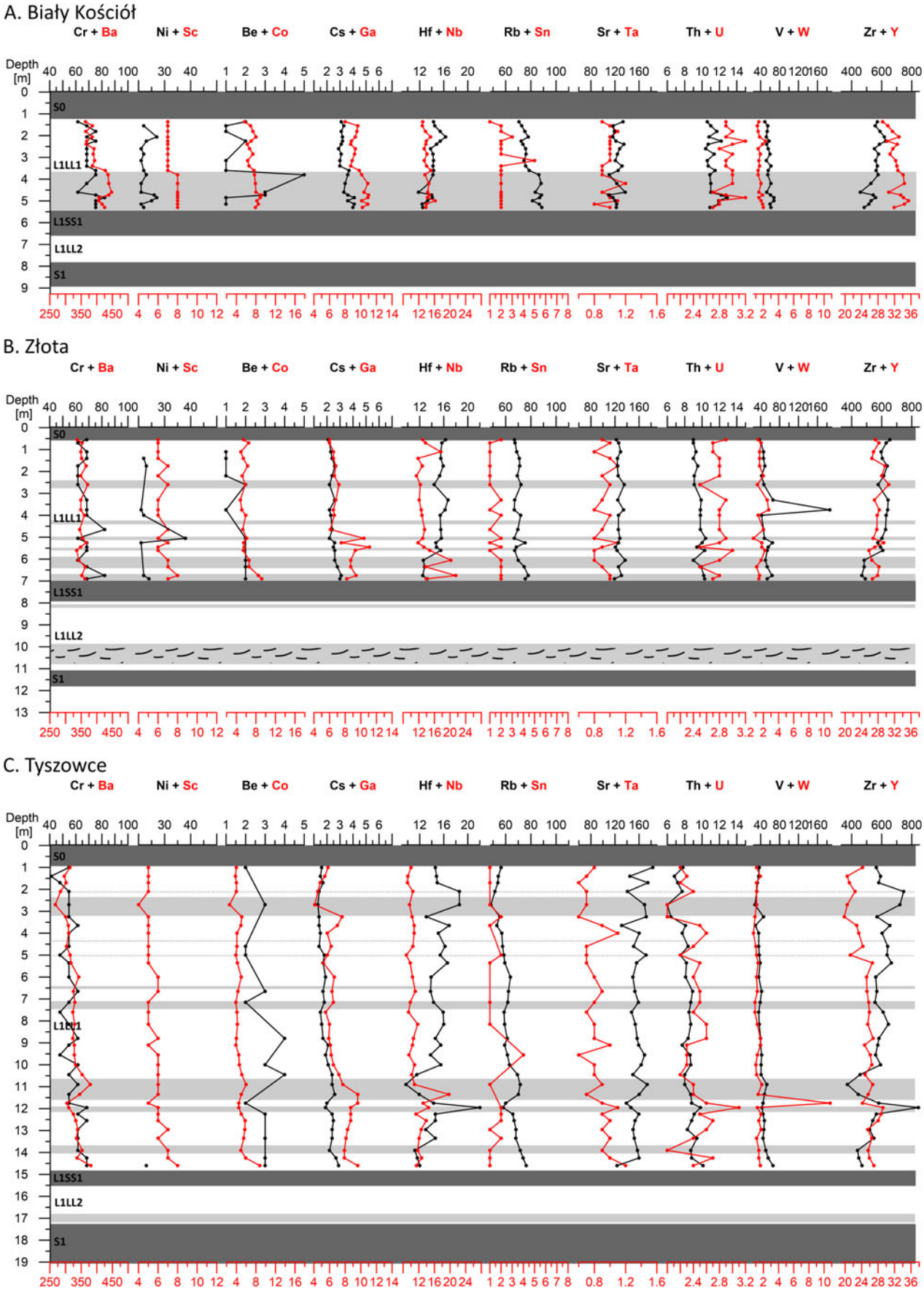

Figure 4. Variability of trace elements (ppm) at the research sites. The main pedo- and lithostratigraphic units are also indicated. See Figure 2 for lithologic legend.

https://doi.org/10.1017/qua.2023.69 Published online by Cambridge University Press

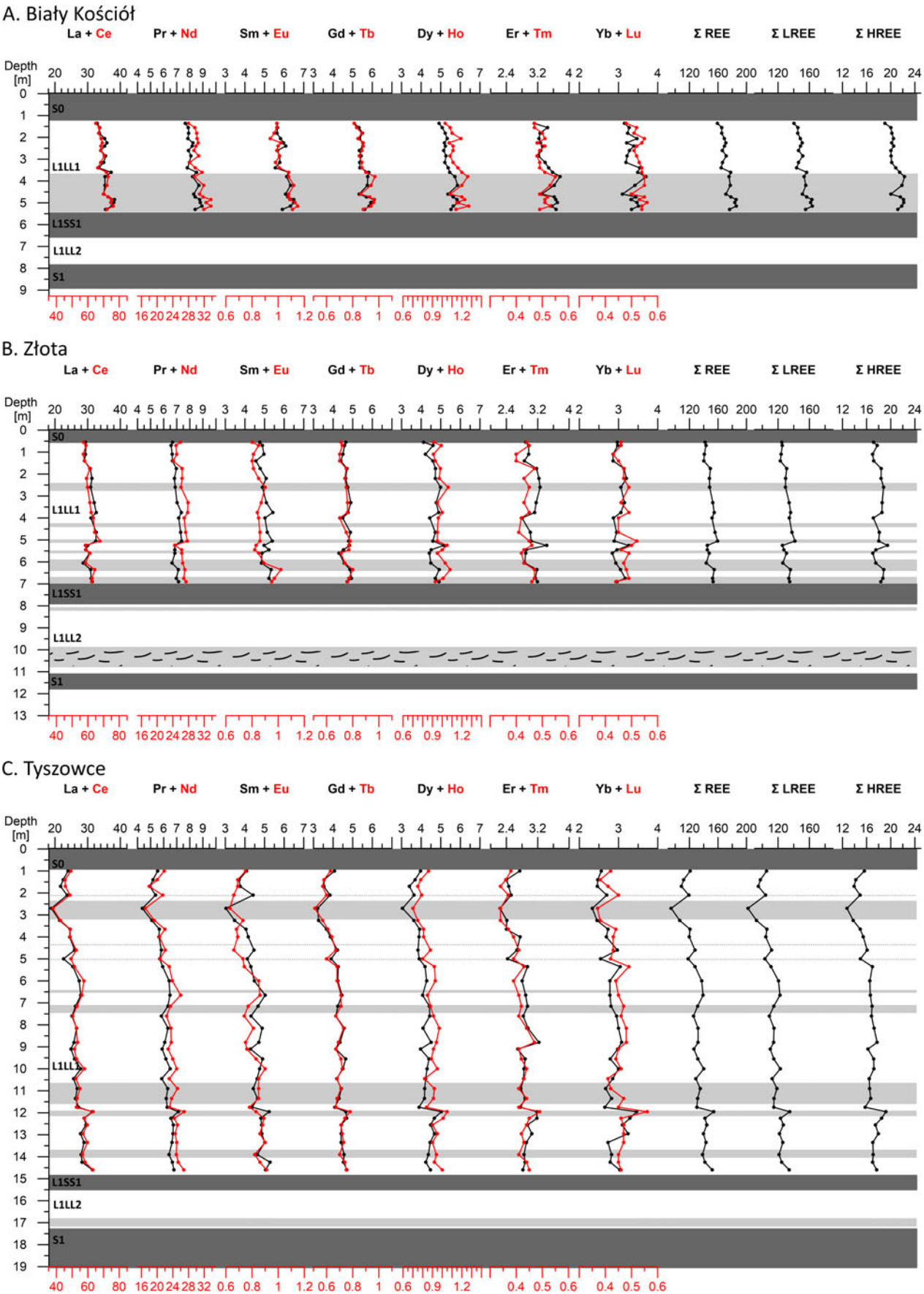

Figure 5. Variability of the rare earth elements (ppm) at the research sites. The main pedo- and lithostratigraphic units are also indicated. See Figure 2 for lithologic legend.

https://doi.org/10.1017/qua.2023.69 Published online by Cambridge University Press

soils on the chemical composition was found, except for a few horizons at Tyszowce (Fig. 3). Even decalcification, one of the first pedogenetic process taking place in loess (Liu, 1985; Jahn et al., 2001; Finke and Hutson, 2008), is not clearly indicated, based on elements associated with carbonates (e.g., CaO or Sr). Conversely, the lower parts of the L1LL1 are generally enriched in oxides of the major elements (Figs. 3–5) such as aluminum (Al_2O_3). Al_2O_3 is strongly positively relative to the iron (Fe_2O_3; Spearman's rank correlation coefficient is 0.63 at Złota, 0.93 at Biały Kościół, and 0.99 at Tyszowce), which is one of the most mobile elements in humid-climate soils. Nonetheless, it has to be noted that iron mobility varies with conditions such as redox potential, the presence of organic matter, or the type of mineral phases (Kabata-Pendias and Pendias, 1999). TiO_2 also shows tendencies similar to Al_2O_3 and Fe_2O_3 (Fig. 3; e.g., at Tyszowce the Spearman's rank correlation coefficient between Al_2O_3 and TiO_2 is 0.81). This is of particular interest because TiO_2 is unlikely to migrate due to the very low solubility of its compounds (e.g., Sheldon and Tabor, 2009), and is consequently transported passively in the form of primary minerals or in secondary products of weathering (Kabata-Pendias and Pendias, 1999). In reducing and acidic environments and in the presence of organic matter, TiO_2 is partially mobile and enters the structure of clay minerals (Kabata-Pendias and Pendias, 1999). Increases in the contents of TiO_2, Al_2O_3, and Fe_2O_3 with depth (or simply in the deeper parts of the L1LL1 units) are likely driven by a greater share of clay minerals or amorphous hydroxides (Kabata-Pendias and Pendias, 1999; Reeder et al., 2006) in the source material (likely the older loess, which has been eroded and re-deposited from neighboring areas; e.g. Kemp, 2001; Jeong et al., 2008; Mroczek, 2013; Skurzyński et al., 2020) and not by post-depositional changes.

Interpretations based on correlations between oxides (in percentages) seem reasonable, however they may be faced with the closed-array compositional conundrum (i.e., the increase in one oxide necessitates a decrease in at least one other element, resulting in spurious negative correlations; Chayes, 1971; Templ et al., 2008; Rollinson, 2013; Andrews et al., 2023). Therefore, additional analyses were based on geochemical indicators and diagrams, which should not be significantly affected by the selective removal or enrichment effect (e.g., Buggle et al., 2008). One of them is the chemical index of alteration (CIA; Nesbitt and Young, 1982), which is illustrated (Figs. S3–S5) on the A–CN–K diagrams (Nesbitt and Young, 1984).

The CIA for the entire loess–paleosol sequence at Złota (including the majority of samples taken from loess L1LL2 and paleosol L1SS1, correlated to MIS 4 and MIS 3, respectively) ranges between 50–65 (Fig. S3; Skurzyński et al., 2020), with only some samples having experienced moderate weathering (65–85). These data suggest that the site has undergone weak chemical weathering under a cold and dry climate (e.g., Song et al., 2014) and periodic warm and moist paleoclimatic conditions for some of the soil samples (Fig. S3). Considering only L1LL1 loess from Złota, the majority of samples are tightly clustered close to the CIA value of 50, which is characteristic for unweathered crustal rocks (Nesbitt and Young, 1982, 1984). Additionally, the lowermost part of the L1LL1 (6.35–6.75 m) is slightly more weathered (similar to the L1LL2 unit) (Figs. 6 and S3).

At Biały Kościół, samples from the L1LL1 unit (Figs. 6 and S4) are less clustered than at Złota (Figs. 6 and S3). The loess collected in the lowest part (4.73–5.3 m), above the L1SS1 soil, is the most weathered, and the loess collected from highest part of all the samples (1.36 m) has the lowest CIA value (Fig. S4). These data illustrate the typical decreasing degree of chemical weathering upward in the profile. However, there are some samples from higher parts of the profile (1.55 m and, to a lesser extent, 1.81 and 2.06 m) that are relatively more weathered and enriched with K_2O (Fig. S4, Table S2). This may suggest the downward penetration of pedogenic effects (e.g., Han et al., 2019) and use of fertilizers, which are the main anthropogenic source of potassium (e.g., Reeder et al., 2006). The least-weathered samples are poorer in K_2O than other samples (Fig. S4). In turn, the lower part of the profile (3.8–5.3 m) is also rich is K_2O, which may be related to the enrichment in fine granulometric fractions (Table S2)—the very soluble simple cation K^+, derived from weathered potassium feldspars, may be easily incorporated into the crystal lattice of clay minerals or adsorbed on them (e.g., Reeder et al., 2006). Because K-bearing mineral phases (such as potassium feldspars) are quite resistant to chemical weathering (e.g., Wilson, 2004), post-depositional processes cannot be the dominant factor determining its variability in the investigated profile. Given the environmental conditions this site experiences, feldspar breakdown is unlikely to be the key driver of potassium variability; a change in the source material is more likely the cause. However, taking into account the range of infiltration (2–5 m; Tu et al., 2009; Zeng et al., 2016) and potential rapid transportation of rainwater through cracks (Derbyshire, 2001), secondary enrichment cannot be ruled out.

At Tyszowce (Fig. S5) the samples taken from the deformation levels and/or initial soil horizons (11.35 m, 12.95 m, or 14.6 m below ground level) clearly deviate from 'the freshest' loess within the L1LL1 unit (e.g., 1.4 m, 8.15 m, or 9.55 m below ground level). These data may indicate changing paleoenvironmental conditions (pure loess deposition vs post-depositional initial pedogenesis) during the formation of this very thick loess unit (Jary, 2007; Moska et al., 2017; Skurzyński et al., 2019). On the other hand, the lowest CIA values are associated with layers enriched with sand (Fig. S5; Skurzyński et al., 2019), suggesting that the chemical composition here is controlled by the mutual proportion of the finer- and coarser-grained materials.

Factors controlling the spatial variability of Polish loess' chemical composition

Most samples, representing the spatial variability of loess in Poland, are weakly weathered (Fig. 6). Only loess samples from Branice oscillate around the CIA value of 65 (Fig. 6), resembling data from the L1SS1 soil at the Złota loess-paleosol sequence (Fig. S3). Considering that samples from Branice are characterized by the finest grain size from the Polish loess (Jary, 2007; Table S3), the effect of granulometric sorting may be a better explanation than different intensities of soil-forming processes (conditioned by different features of the paleoclimate) for variability of CIA values. This conclusion is demonstrated by the A–CN–K diagram, which also reflects the grain-size differentiation (Buggle et al., 2008), with the finest material the closest to the apex of the Al_2O_3 axis (Nesbitt et al., 1996), such as the highest CIA values (Nesbitt and Young, 1984).

The highest values of CIA, as well as the finest material, were found at Branice, and in the lowest parts of the Biały Kościół (4.73–5.3 m), Tyszowce (14.6 m), and Złota (6.75 m) sections (Fig. 6). The remaining (even the freshest) parts of L1LL1 at Biały Kościół (4.6–1.36 m) resemble the lower parts of L1LL1 at

https://doi.org/10.1017/qua.2023.69 Published online by Cambridge University Press

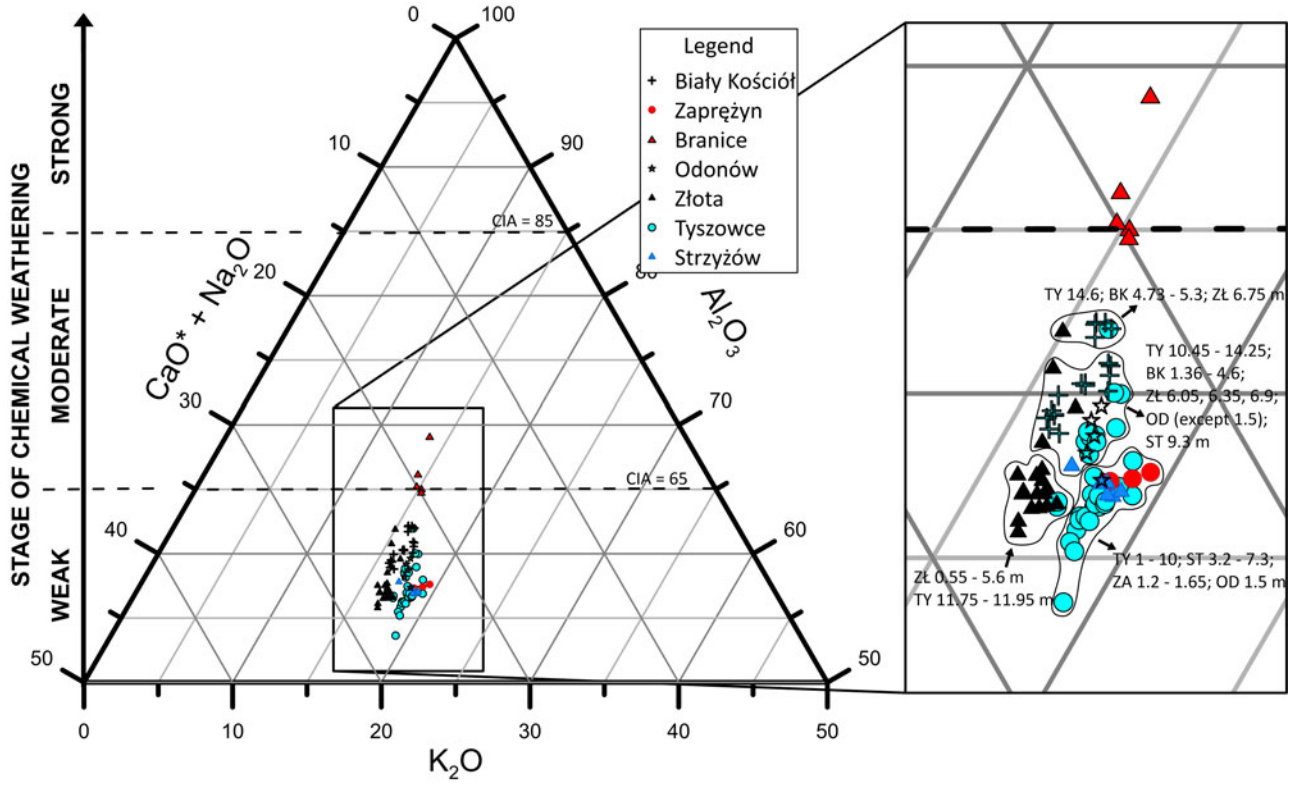

Figure 6. A–CN–K ternary diagram (Nesbitt and Young, 1984) of the Polish loess samples. CaO* (Ca in silicates) was calculated according to McLennan (1993). Dashed lines = CIA values of 65 and 85. Stratigraphical labeling system after Kukla and An (1989), modified by Marković et al. (2008, 2015).

Tyszowce (14.25–10.45 m) or at Złota (6.05, 6.35, and 6.9 m), similar to the loess from Odonów (Fig. 6). In turn, the freshest loess in the whole dataset was found, in general terms, in the upper (and therefore the youngest) parts of loess L1LL1 at Złota (0.55–5.6 m), Tyszowce (1–10 m and 11.75–11.95 m), and at the northern sites (Strzyżów and Zaprężyn) (Fig. 6). Zaprężyn, which is located only ~60 km (straight-line distance) towards the NNE from the profile at Biały Kościół (Fig. 1), is particularly important in this context, given that its weak weathering likely is not the direct result of different paleoclimatic conditions in relation to the Biały Kościół. A better explanation may be so-called loess cannibalism (Van Loon, 2006; Licht et al., 2016) because a hiatus in loess deposition was found at Zaprężyn (from 56.8 ± 4.7 ka to 18.4 ± 1.2 ka; Zöller et al., 2022). The missing loess, theoretically deflated from Zaprężyn, could have been transported southwards and re-deposited at Biały Kościół. It may further suggest that, similar to loess at Biały Kościół, the loess from southern loess deposits (Branice, Odonów), as well as the lowermost parts of the L1LL1 units from eastern loess–paleosol sequences (Tyszowce and Złota), contain sediment eroded and reworked from paleosols or older loess covers that mixed with fresh, incoming dust (Mroczek, 2013). Consequently, the varying proportions of older and fresher material could explain the overall variability of the CIA values (Fig. 6), since the higher supply of fresh material would have led to smaller chemical weathering values (e.g., Varga et al., 2011). In this approach, the last phase of loess deposition in MIS 2 in the study area would have supplied the fresh material to the northern profiles like Zaprężyn (since 18.4 ± 1.2 ka; Zöller et al., 2022) and Strzyżów (substantial deposition since ca. 19 ka; Moska et al., 2019b). That supply of fresh sediment was likely provided mostly from the north, given that loess with higher weathering values occurs in the south. Given the > 6-m-thick layer of loess L1LL1 (3.20–9.30 m) at Strzyżów, and the lack of differentiation of the low CIA values there (Fig. 6), the supply was likely stable and substantial.

A northern source of the material is also suggested by the positive Zr and Hf anomalies (Fig. 7, Table S2), which in Europe are commonly associated with periglacial loess (Rousseau et al., 2014, and the references therein) and limited to material deposited near the Fenno-Scandinavian Ice Sheet (Scheib et al., 2014; Bosq et al., 2020). This confirms the relationship of Polish loess to glaciogenic deposits, since the enrichment with elements related to the chemically resistant minerals, such as zircon (Zr and Hf), may be attributed best to the removal of more weatherable minerals during the processes of glacial grinding and post-depositional leaching in the sub- and proglacial environments of Poland (Lis and Pasieczna, 2006; Buggle et al., 2008). The data also strengthen the previous premise about the relationship between the chemical and grain-size compositions of the loess because zircons are known to be concentrated preferentially in coarse-grained silt and sand fractions in aeolian sediments (Muhs and Bettis, 2000, Yang et al., 2006). The results further demonstrate that all samples (collected both from the main and supplementary research sites) are arranged in accordance with the sedimentary recycling trend line in the Zr/Sc vs Th/Sc diagram (Fig. 8), while the finest-grained material is the most depleted in zircons (Fig. 8).

We conclude that Polish loess can be considered to be generally unweathered sediment, with slight variations in granulometry or weathering history. Therefore, the variability of chemical

https://doi.org/10.1017/qua.2023.69 Published online by Cambridge University Press

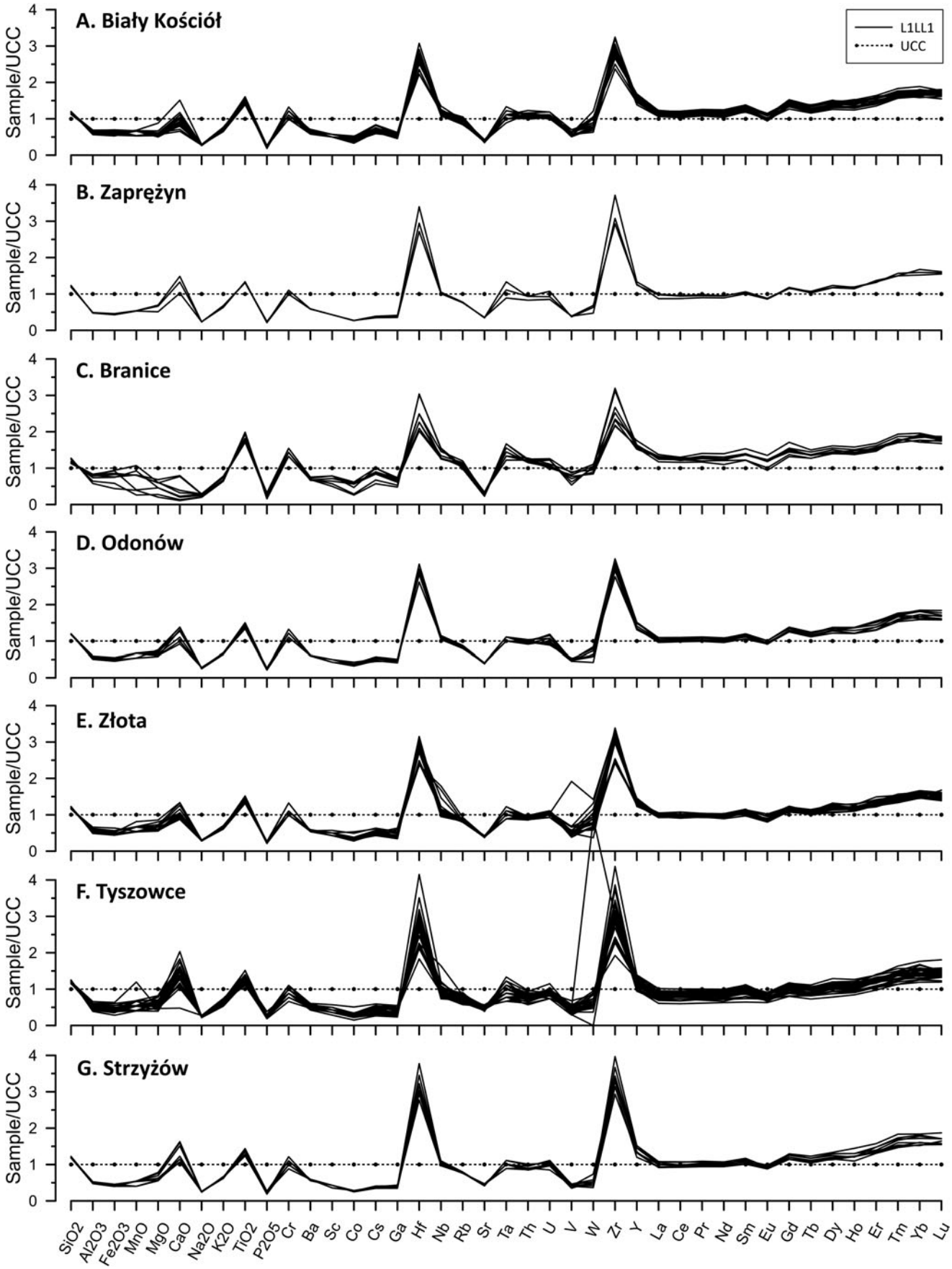

Figure 7. UCC-normalized multielement spidergrams for Polish loess. Each curve represents one sample. Ni is not shown because of its presence only in some samples. The UCC values used are from Rudnick and Gao (2003).

https://doi.org/10.1017/qua.2023.69 Published online by Cambridge University Press

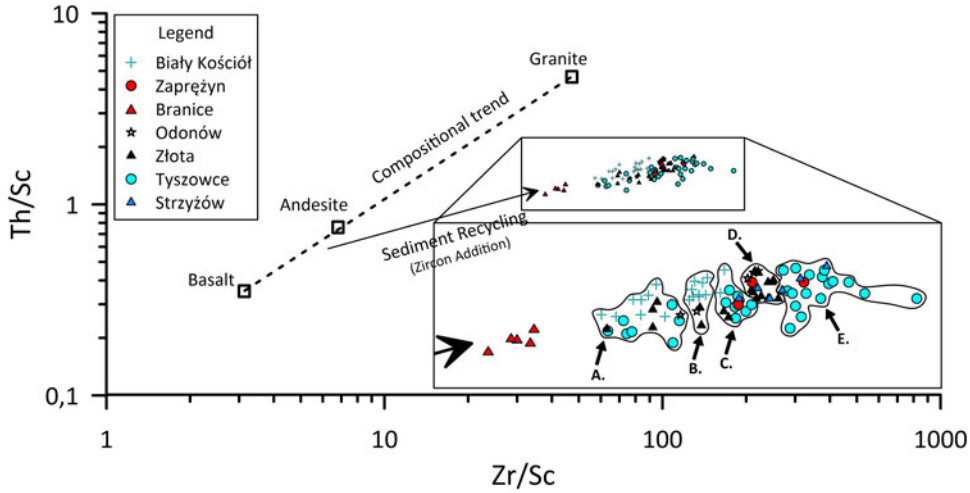

Figure 8. Th/Sc vs Zr/Sc discrimination diagram of sedimentary recycling (McLennan et al., 1993) for Polish loess. Explanations: A = BK 3.8–5.3; ZŁ 6.05–6.9; TY 10.45–11.35, 12.95, and 13.9–14.6; OD 2.5 m. B = BK 1.36–3.6 (except 2.06 and 2.25); ZŁ 2.6 and 5.25; OD 3.3 m. C = BK 2.06 and 2.25; ZŁ 1.75 and 4.65; TY 6–6.65 m, 8.8, 9.55–10, 12.25–12.55, 13.35; ST = 5; ZA = 1.2 m, D = ZŁ 0.55–1.4, 2.2, 3.3–4, 5.05, 5.45–5.6; OD 0.9–1.8; ST 3.2–3.8; ZA–1.5 m. E = TY 1–5.35, 7.15 8.15, 9.1, 11.75–11.95; ST 4.4, 7.3–9.3; ZA = 1.65 m. Zoomed area is not in the scale.

compositions is mostly influenced by the enrichment and depletion of the silica, carbonates, and secondary weathering products (Gallet et al., 1998). In essence, the duration of post-depositional processes has not been long and intense enough to mask the chemical signature of the loess parent material (Campodonico et al., 2019; Skurzyński et al., 2020). Of course, admixtures of local material also may be important (e.g., the highest share of carbonates at Tyszowce probably relates to the local bedrock, which is limestone; Maruszczak, 1991).

General homogeneity of Polish loess' chemical composition

The overall homogeneity of Polish loess is suggested by the very similar shape of the UCC-normalized diagrams for all of the investigated sites (Fig. 7). Particularly important is the slight variation in REE curves because the magmatic or metamorphic rocks (the protolith of all the loess sediments) have a much greater diversity, and the only way to average all these to a nearly constant pattern is by recycling and mixing during at least one cycle of sedimentary processes (Gallet et al., 1998). The statistically significant differences (Table S4) of absolute abundances of chemical elements and oxides are not particularly important for the geochemical indices, based on the trace element composition (e.g., Th/U: 2.96–4.63; median 3.56), the lack of distinct Ce anomaly (0.96–1.08; median 1.00), or the relatively stable values of La_N/Sm_N (3.34–4.06; median 3.78), La_N/Yb_N (5.48–8.10; median 6.69), and Gd_N/Yb_N (1.08–1.49; median 1.26). These all suggest an indistinguishable REE fractionation between unweathered and weathered loess due to relatively greater mobilization of heavy REE (HREE) than light REE (LREE). The significant weathering would lead to a decrease in La_N/Sm_N values, and an increase in La_N/Yb_N and Gd_N/Yb_N values (Nesbitt, 1979; Hao et al., 2010; Han et al., 2019; Skurzyński et al., 2020).

PML – Polish median loess

The weakly weathered (Fig. 6) Polish loess is geochemically homogeneous, relative to published data on loess from around the world (e.g., Pye, 1984; Rousseau et al., 2014; Bosq et al., 2020). Thus, it may be important for paleoenvironmental interpretations, because trace elements and rare earth elements are widely used to infer the provenance of sediments (Li et al., 2021; Shi et al., 2023), but the differences may be relatively minor, and for the different loess deposits the REE patterns in the normalized diagrams are hardly distinguishable (Guo, 2010). For example, the HREE patterns may be a good overall indicator of loess diversity in Europe (Skurzyński et al., 2020). Thus, Gd_N/Yb_N values of Polish loess were tested against the background of samples from various European loess areas (Fig. 9). To avoid comparing differences related to adopted research methodology (Skurzyński and Fenn, 2022) only studies that used similar approaches were utilized (Rousseau et al., 2014; Bosq et al., 2020). Additionally, a cross-analysis of the Gd_N/Yb_N was carried out (for Tyszowce and Złota: Bosq et al., 2020 vs this study; and for Surduk: Rousseau et al., 2014 vs Bosq et al., 2020). For the loess sample from Tyszowce analyzed by Bosq et. al. (2020), the value of Gd_N/Yb_N was 1.13 (this study: median 1.18, min. 1.08, max. 1.35) and for Złota, the value of Gd_N/Yb_N was 1.17 (this study: median 1.26, min. 1.18, max. 1.34). The Gd_N/Yb_N for the Surduk profile (located in Serbia) was 1.43, according to Bosq et al. (2020), and 1.55, according to Rousseau et al. (2014). For Polish loess, the values of Gd_N/Yb_N are visibly lower than the loess in Surduk, which is understandable because these loess deposits have different sources. Similarly, low values like in Polish loess were found (Fig. 9) in the English Channel, Ukraine (Stayky, Korshiv), eastern Germany (Ostrau, Zeuchfeld), and Aquitaine (Pomarez). Even for the most weathered Polish loess (Branice; Fig. 9), the median of Gd_N/Yb_N is lower than reported by Bosq et al. (2020), but comparable to the median from Rousseau et al. (2014).

Even relatively small differences in the values of appropriately chosen parameters between Polish loess and loess from other regions can be detected, and therefore infer important information about the source of the material. However, these kinds of minor differences are often imperceptible due to the UCC normalization, which is very common in the literature. This set of chemical data is unsuited to the specificity of loess. For this reason, many elements create very clear positive or negative

https://doi.org/10.1017/qua.2023.69 Published online by Cambridge University Press

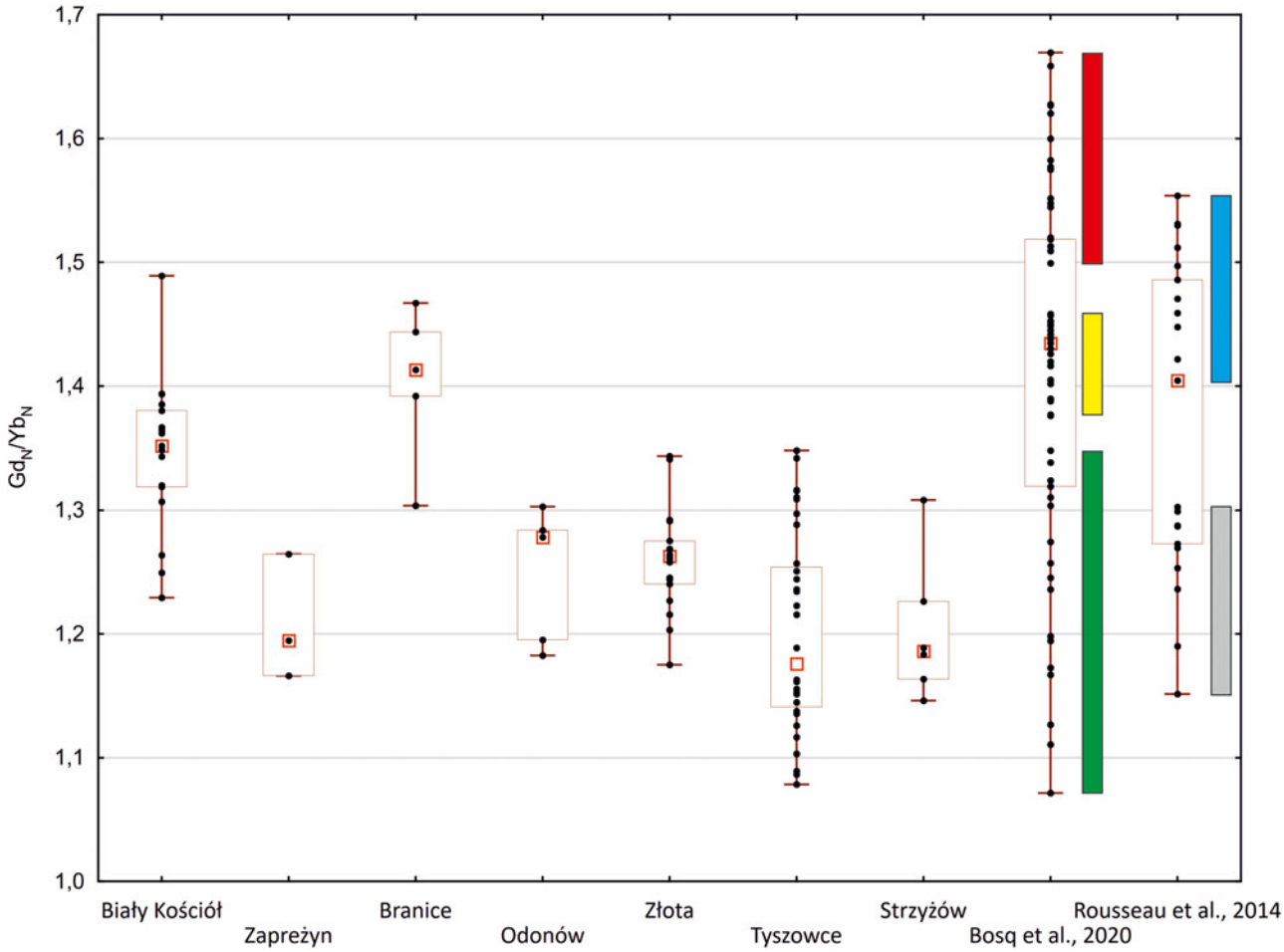

Figure 9. Box plots of Gd_N/Yb_N values of Polish and European loess; red squares = medians; whiskers = ranges of values; frames = 25–75% of values. Explanations of data from literature (colored polygons): red rectangle (data from Bosq et al., 2020) shows samples from Rhine (Achenheim, Nussloch) and Rhône (Baix, Bouzil, Brillanne, Collias, Cuges les Pins, Donnat, Lautagne, Mauves, Pact, Serezin du Rhône, Saint Julien de Peyrolas, Saint Paul les Durance, Vaise); yellow rectangle (data from Bosq et al., 2020) shows samples from northern France (Quesnoy, Hauteville), Germany–Saxony (Rottewitz), Rhine (Schaffhouse), Serbia (Surduk), Rhône (Feyzin, Garons, Lautagne, Ledenon, Montanay, Saint-Péray, Sathonay, Saint Cyr au Mont d'Or, Saint-Désirat, Saint Georges les Bains, Soyons, Tain l'Hermitage); green rectangle (data from Bosq et al., 2020) shows samples from northern France (Beutin, Glos, Nisy le Comte, Sourdon, Verlinghem, Chaudon, Havrincourt, Renancourt, Villers Carbonnel), Aquitaine (Pomarez, Romentères), Belgium (Harmignies), Ukraine (Korshiv), eastern Germany (Ostrau), Poland (Tyszowce, Złota); blue rectangle (data from Rousseau et al., 2014) shows samples from western Germany (Nussloch; samples from following depths: 5, 6, 7.9, 9.5, 10.3, 12, 14.1, 17.8 m), western Europe (Pleneuf Val Andre, Languevoisin), Serbia (Surduk); gray rectangle (data from Rousseau et al., 2014) shows samples from western Europe (English Channel, Villers Carbonel, Harmignies), eastern Germany (Gleina, Leippen, Ostrau, Seilitz, Zehren, Zeuchfeld), Ukraine (Stayky).

anomalies on the UCC-normalized diagrams (Fig. 7). Therefore, a set of normalization data dedicated to loess could be used, such as AVL[1] (Schnetger, 1992; modified by Újvári et al., 2008) or GAL (Újvári et al., 2008). However, these normalizing sets are based on the results obtained using variable methods, from samples representing diverse worldwide loess regions, and showing values for limited number of elements (most trace elements and REEs are omitted). An additional complication is the fact that even in a not very large group of loess normalization data sets, the same average loess may be presented in different scope and under different names. A good example is way that the average loess, introduced by Schnetger (1992) and cited later as AVL[1] by Újvári et al. (2008), is limited to the selected chemical elements. This may cause some confusion, so the name AVL[1] has been consistently used in this work (Újvári et al., 2008); however, Table 1 presents the complete set of elements from the original average loess (Schnetger, 1992). The relevant information can be found in the caption of Table 1.

Therefore, we propose a new parameter – Polish median loess (PML), based on data obtained by same methods, from one loess region with a homogeneous and fresh chemical composition, such as Poland. Moreover, the PML dataset represents a nearly complete range of variability of chemical composition of loess deposited at a similar time (MIS 2, as shown by numerous OSL ages), although differing in granulometric composition. The PML is based on medians of individual elements, not average values, and for this reason, it is insensitive to outlier values that remain in the data set (the paleoenvironmental information related to them was not lost).

The PML is determined in wt. %, on a volatile-free basis, for oxides of major elements, and in ppm for trace elements and REEs. The PML values are clearly different from previously published average loess compositions (GAL and AVL[1]; Table 1), but show some similar trends to them, such as higher values of elements related to chemically and mechanically resistant mineral phases (e.g., SiO_2, Hf, Zr) in relation to the UCC (Table 1). The

https://doi.org/10.1017/qua.2023.69 Published online by Cambridge University Press

Table 1. Polish median loess (PML; this study) versus UCC (Rudnick and Gao, 2003), AVL[1] (Schnetger, 1992; Újvári et al., 2008), however the AVL[1] presented by Újvári et al., 2008, lacks the values for Co, Cs, Hf, Ta, U, W, Pr, Nd, Sm, Eu, Gd, Tb, Dy, Ho, Er, Tm, Yb, and Lu, so these elements are cited after original average loess presented by Schnetger (1992), and GAL (Újvári et al., 2008). Major elements (wt.%) are recalculated on a volatile-free basis. Total iron is expressed as Fe_2O_3 (Fe_2O_3 value of AVL[1] in this study was recalculated from $FeO_{(tot)}$ = 2.78% as presented by Újvári et al., 2008). Schnetger (1992) reported FeO (= 0.8%) and Fe_2O_3 (= 2.2%) separately. Trace elements and REE are in ppm. The color scale was developed using the conditional formatting function of MS Excel: the red–yellow–green color scale indicates the position of a given value in the entire range of values in a given column (red = high values; yellow = medium values; green = low values). N/D means no data.

	PML	UCC	AVL[1] *	GAL
SiO_2	78.64	66.00	76.50	70.71
Al_2O_3	8.19	15.20	12.50	11.74
Fe_2O_3	2.41	5.00	3.09	3.75
MgO	1.32	2.20	1.00	2.15
CaO	4.81	4.20	1.30	6.67
Na_2O	1.07	3.90	2.10	1.68
K_2O	2.25	3.40	2.30	2.22
TiO_2	0.68	0.50	0.63	0.71
P_2O_5	0.10	0.40	N/D	0.14
MnO	0.04	0.08	0.06	0.07
Cr	68.42	62.00	43.00	67.00
Ba	360.00	628.00	582.00	427.00
Ni	22.00	47.00	18.00	27.00
Sc	6.00	14.00	8.00	N/D
Co	5.50	17.30	9.00	N/D
Cs	2.40	4.90	3.70	N/D
Ga	7.90	17.50	13.00	12.00
Hf	14.60	5.30	12.00	N/D
Nb	12.80	12.00	18.00	14.00
Rb	69.20	84.00	81.00	79.00
Sr	131.10	320.00	246.00	208.00
Ta	0.90	0.90	1.30	N/D
Th	9.50	10.50	10.00	9.00
U	2.70	2.70	2.60	N/D
V	46.00	97.00	66.00	N/D
W	1.4	1.90	1.30	N/D
Zr	576.2	193.00	387.00	322
Y	27.8	21.00	25.00	26
La	30.8	31.00	35.00	29
Ce	59.8	63.00	78.00	61
Pr	6.86	7.10	8.40	N/D
Nd	26.3	27.00	33.00	N/D
Sm	5.01	4.70	6.40	N/D
Eu	0.88	1.00	1.20	N/D
Gd	4.69	4.00	4.80	N/D
Tb	0.75	0.70	0.80	N/D
Dy	4.68	3.90	4.70	N/D
Ho	0.99	0.83	1.00	N/D
Er	3.06	2.30	2.80	N/D
Tm	0.45	0.30	N/D	N/D
Yb	3.08	1.96	2.70	N/D
Lu	0.48	0.31	N/D	N/D

differences between PML and UCC (Table 1) seem more important, because the latter is widely used. We next tested the new loess-dedicated normalization data set against two loess samples from different regions (Ukraine and Serbia; Bosq et al., 2020) and compared with UCC-normalized data via multielement spidergrams (Fig. 10).

The UCC-normalization of the Korshiv (Ukraine) section shows numerous positive and negative anomalies, while PML-normalization illustrates that loess from Korshiv is only slightly enriched in MnO, MgO, CaO, and Sr, as compared to Polish loess (Fig. 10). Conversely, Serbian loess has higher values of almost all elements and oxides in relation to the Polish loess, which is much more visible than in the case of UCC-normalization (Fig. 10). This suggests that the use of PML may highlight even the barely noticeable differences between loess regions in Europe. It may also facilitate the cross-continental comparative analysis of loess geochemical compositions. We note that, for this type of analysis, the focus traditionally has been on Asian and North American loess (e.g., Muhs, 2018).

By developing the PML we hope that other regional reference datasets (e.g., for China, USA, Argentina) will be developed using similar methods, which will allow for further geochemical comparisons. Until then, PML remains a reliable and comprehensive dataset for loess normalization elsewhere.

CONCLUSIONS

The geochemical compositions of the youngest (MIS 2) Polish loess units (L1LL1) are clearly differentiated in vertical profiles. However, the classic chemostratigraphy, based on analyses of the variability of individual elements (or their correlations) with depth, is not always suitable for loess deposited in a dynamic periglacial environment. The more effective way to examine this loess is to use geochemical diagrams, which should not be significantly affected by a selective removal or enrichment effect, or by the effect of closed-array compositional conundrum, which may result in spurious negative correlations.

The analysis of chemical weathering in the loess showed that the most-weathered sites are located in the southern part of Poland, as well as the lowest parts of the sections in the north. The freshest loess was found, in general terms, in the upper (and therefore the youngest) parts of the L1LL1 loess at Złota, Tyszowce, Strzyżów, and Zaprężyn. The comparatively weak weathering data for loess at Zaprężyn changes the earlier assumptions about a clear division of the Polish loess area into more weathered loess of western Poland and relatively fresh loess of eastern Poland. The profiles located in the northern part of the research area (both in the east and in the west) are much fresher than the profiles in the southern sector of Poland. The most reasonable explanation seems to be deflation and transportation of the older material southwards and later depositing it at the Biały Kościół or Branice areas. As a consequence, there is no older material more northward (e.g., at Zaprężyn) where the fresh material was deposited.

Nonetheless, despite statistically significant differences in the degree of chemical weathering, as well as in the other geochemical parameters and indices, the general homogeneity (or the well-mixed nature) of Polish loess is clearly visible and has been demonstrated for each of the research sites. The loess is relatively fresh, was thoroughly mixed and homogenized during transportation and/or sedimentary recycling, and has not been significantly affected by post-depositional processes or admixture of the local material.

The overall homogeneity of the Polish loess studied here has allowed for the calculation of a new, loess-normalizing dataset named Polish median loess (PML). These data may be of particular importance for comparative analyses of loess from different

https://doi.org/10.1017/qua.2023.69 Published online by Cambridge University Press

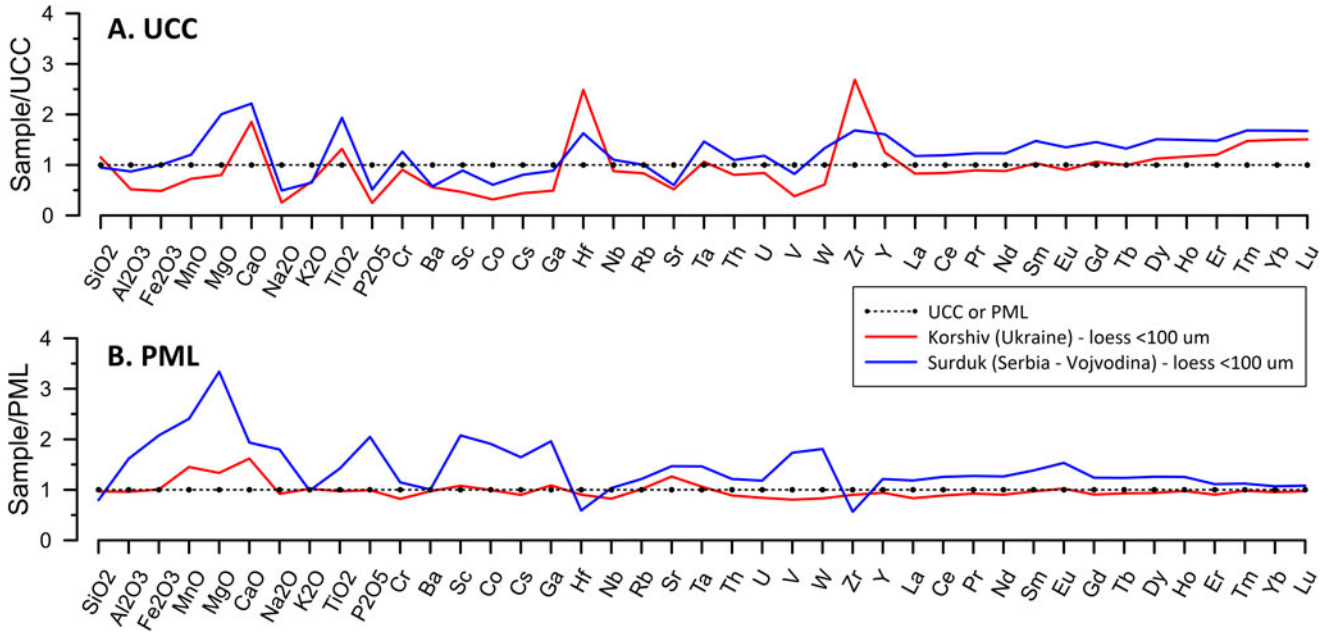

Figure 10. UCC-normalized and PML-normalized multielement spidergrams for loess samples from Korshiv (Ukraine) and Surduk (Serbia) (geochemical data used for normalization after Bosq et al., 2020). Each curve represents one sample. Ni is not shown because of its presence only in some samples. The UCC values used are from Rudnick and Gao (2003), PML values are from this study.

parts of the world. The PML also may constitute the basis for further work on a pan-European or even global reference dataset, thus maintaining rigor in the research methodology used and in the selection of research sites and samples.

Appendix A. Supplementary data. Supplementary data to this article can be found online at https://doi.org/10.1017/qua.2023.69

Acknowledgments. The geochemical research was performed under the National Science Centre project No. 2017/27/N/ST10/01208 entitled "Stratigraphic and spatial variability of the chemical composition of Late Pleistocene loess-soil sequences of Poland in the context of palaeoenvironmental and palaeoclimatic changes" (Principal Investigator: Jacek Skurzyński); and under the project No. 2017/27/B/ST10/01854 entitled "Sudden COLD events of the Last Glacial in the central part of the European LOESS Belt – in Poland and in the western part of Ukraine (COLD LOESS)" (Principal Investigator: Zdzisław Jary). We are grateful to editors (Nicholas Lancaster and Randal Schaetzl) and two anonymous reviewers for their constructive comments and suggestions.

REFERENCES

Andrews, J.T., Roth, W.J., Jennings, A.E., 2023. Grain size and mineral variability of glacial marine sediments. *Journal of Sedimentary Research* **93**, 37–49.

Badura, J., Jary, Z., Smalley, I., 2013. Sources of loess material for deposits in Poland and parts of Central Europe: the lost big river. *Quaternary International* **296**, 15–22.

Baykal, Y., Stevens, T., Engstrom-Johansson, A., Skurzyński, J., Zhang, H., He, J., Lu, H., Adamiec, G., Költringer, C., Jary, Z., 2021. Detrital zircon U–Pb age analysis of last glacial loess sources and proglacial sediment dynamics in the Northern European Plain. *Quaternary Science Reviews* **274**, 107265. https://doi.org/10.1016/j.quascirev.2021.107265.

Bitelli, M., Andrenelli, M.C., Simonetti, G., Pellegrini, S., Artioli, G., Piccoli, I., Morari, F., 2019. Shall we abandon sedimentation methods for particle size analysis in soils? *Soil and Tillage Research* **185**, 36–46.

Bosq, M., Bertran, P., Degeai, J-P., Queffelec, A., Moine, O., 2020. Geochemical signature of sources, recycling and weathering in the last glacial loess from the Rhône Valley (southeast France) and comparison with other European regions. *Aeolian Research* **42**, 100561. https://doi.org/10.1016/j.aeolia.2019.100561.

Buggle, B., Glaser, B., Zoeller, L., Hambach, U., Marković, S., Glaser, I., Gerasimenko, N., 2008. Geochemical characterization and origin of southeastern and Eastern European loesses (Serbia, Romania, Ukraine). *Quaternary Science Reviews* **27**, 1058–1075.

Buggle, B., Glaser, B., Hambach, U., Gerasimenko, N., Marković, S., 2011. An evaluation of geochemical weathering indices in loess–paleosol studies. *Quaternary International* **240**, 12–21.

Butrym, J., 1987. TL ages for loess profile in Odonów near Kazimierza Wielka. In: Madeyska, T. (Ed.), *Scientific Research Report of Committee of Quaternary Research of the Polish Academy of Science* **7**, 10–15.

Campodonico, V., Rouzaut, S., Pasquini, A., 2019. Geochemistry of a late Quaternary loess–paleosol sequence in central Argentina: implications for weathering, sedimentary recycling and provenance. *Geoderma* **351**, 235–249.

Cegła, J., 1972. Sedymentacja lessów Polski. *Acta Universitatis Wratislaviensis* **168**, 71 pp. [in Polish]

Chayes, F., 1971. *Ratio Correlation*. University of Chicago Press, Chicago, 99 pp.

Condie, K.C., 1993. Chemical composition and evolution of the upper continental crust: contrasting results from surface samples and shales. *Chemical Geology* **104**, 1–37.

Derbyshire, E., 2001. Geological hazards in loess terrain, with particular reference to the loess regions of China. *Earth Science Reviews* **54**, 231–260.

Ebens, R.J., Connor, J.J., 1980. Geochemical survey of Missouri – geochemistry of loess and carbonate residuum. *U.S. Geological Survey Professional Paper*, 954-G, 32 pp.

Fenn, K., Prud'homme, C., 2022. Dust deposits: loess. In: Schroder, J.F., Lancaster, N. (Eds.), *Treatise on Geomorphology*. Elsevier, Amsterdam, pp. 320–365.

Fenn, K., Thomas, D.S.G., Durcam J.A., Millar, I.L., Veres, D., Piermattei, A., Lane, C.S., 2021. A tale of two signals: global and local influences on the Late Pleistocene loess sequences in Bulgarian Lower Danube. *Quaternary Science Reviews* **274**, 107264. https://doi.org/10.1016/j.quascirev.2021.107264.

Fenn, K., Millar, I.L., Durcan, J.A., Thomas, D.S.G., Banak, A., Marković, S.B., Veres, D., Stevens, T., 2022. The provenance of Danubian loess.

Earth-Science Reviews **226**, 103920. https://doi.org/10.1016/j.earscirev.2022.103920.

Finke, P., Hutson, J.L., 2008. Modelling soil genesis in calcareous loess. *Geoderma* **145**, 462–479.

Gallet, S., Jahn, B.-M., Van Vliet Lanoë, B., Dia, A., Rossello, E., 1998. Loess geochemistry and its implications for particle origin and composition of the upper continental crust. *Earth and Planetary Science Letters* **156**, 157–172.

Guan, H., Zhu, C., Zhu, T., Wu, L., Li, Y., 2016. Grain size, magnetic susceptibility and geochemical characteristics of the loess in the Chaohu Lake basin: implications for the origin, paleoclimatic change and provenance. *Journal of Asian Earth Sciences* **117**, 170–183.

Guo, Z., 2010. Loess geochemistry and Cenozoic paleoenvironments. *Geochemical News* **143**, 1–10.

Han, L., Hao, Q., Qiao, Y., Wang, L., Peng, S., Li, N., Gao, X., Xu, B., Gu, Z., 2019. Geochemical evidence for provenance diversity of loess in southern China and its implications for glacial aridification of the northern subtropical region. *Quaternary Science Reviews* **212**, 149–163.

Hao, Q., Guo, Z., Qiao, Y., Xu, B., Oldfield, F., 2010. Geochemical evidence for the provenance of middle Pleistocene loess deposits in southern China. *Quaternary Science Reviews* **29**, 3317–3326.

Jahn, A., 1950. Loess, its origin and connection with the climate of the glacial epoch. *Acta Geologica Polonica* **1**, 257–310. [in Polish, with English summary]

Jahn, B., Gallet, S., Han, J., 2001. Geochemistry of the Xining, Xifeng and Jixian sections, Loess Plateau of China: eolian dust provenance and paleosol evolution during the last 140 ka. *Chemical Geology* **178**, 71–94.

Jary, Z., 2007. Record of Climate Changes in Upper Pleistocene Loess–Soil Sequences in Poland and Western Part of Ukraine. *Rozprawy Naukowe Instytutu Geografii i Rozwoju Regionalnego Uniwersytetu Wrocławskiego* 1. Wrocław, Poland. [in Polish, with English Abstract]

Jary, Z., Ciszek, D., 2013. Late Pleistocene loess–palaeosol sequences in Poland and western Ukraine. *Quaternary International* **296**, 37–50.

Jeong, G., Hillier, S., Kemp, R., 2008. Quantitative bulk and single-particle mineralogy of a thick Chinese loess–paleosol section: implications for loess provenance and weathering. *Quaternary Science Reviews* **27**, 1271–1287.

Jersak, J., 1973. Lithology and stratigraphy of the loess on the Southern Polish Uplands. *Acta Geographica Lodziensia* **32**, 1–139. [in Polish, with English Abstract]

Kabata-Pendias, A., Pendias, H., 1999. *Biogeochemia Pierwiastków Śladowych*. Wydawnictwo PWN, Warszawa, 398 pp. [in Polish]

Kemp, R.A., 2001. Pedogenic modification of loess: significance for palaeoclimatic reconstructions. *Earth-Science Reviews* **54**, 145–156.

Költringer, C., Stevens, T., Lindner, M., Baykal, Y., Ghafarpour, A., Khormali, F., Taratunina, N., Kurbanov, R., 2022. Quaternary sediment sources and loess transport pathways in the Black Sea–Caspian Sea region identified by detrital zircon U–Pb geochronology. *Global and Planetary Change* **209**, 103736. https://doi.org/10.1016/j.gloplacha.2022.103736.

Konert, M., Vandenberghe, J., 1997. Comparison of laser grain size analysis with pipette and sieve analysis: a solution for the underestimation of the clay fraction. *Sedimentology* **44**, 523–535.

Krawczyk, M., Ryzner, K., Skurzyński, J., Jary, Z., 2017. Lithological indicators of loess sedimentation of SW Poland. *Contemporary Trends in Geoscience* **6**, 94–111.

Kukla, G., An, S., 1989. Loess stratigraphy in central China. *Palaeogeography, Palaeoclimatology, Palaeoecology* **72**, 203–225.

Lehmkuhl, F., Zens, J., Krauß, L., Schulte, P., Kels, H., 2016. Loess–paleosol sequences at the northern European loess belt in Germany: distribution, geomorphology and stratigraphy. *Quaternary Science Reviews* **153**, 11–30.

Lehmkuhl, F., Nett, J.J., Potter, S., Schulte, P., Sprafke, T., Jary, Z., Antoine, P., *et al.*, 2021. Loess landscapes of Europe – mapping, geomorphology, and zonal differentiation. *Earth-Science Reviews* **215**, 103496. https://doi.org/10.1016/j.earscirev.2020.103496.

Li, Z., Chen, Q., Dong, S., Zhang, D., Yu, X., Zhang, C., 2021. Applicability of rare earth elements in eolian sands from desert as proxies for provenance: a case study in the Badain Jaran Desert, northwestern China. *Catena* **207**, 105647. https://doi.org/10.1016/j.catena.2021.105647.

Licht, A., Pullen, A., Kapp, P., Abell, J., Giesler, N., 2016. Eolian cannibalism: reworked loess and fluvial sediment as the main sources of the Chinese Loess Plateau. *GSA Bulletin* **128**, 944–956.

Lis, J., Pasieczna, A., 2006. Geochemical characteristics of soil and stream sediment in the area of glacial deposits in Europe. In: Tarvainen, T., De Vos, W. (Eds.), *Geochemical Atlas of Europe. Part 2. Interpretation of Geochemical Maps, Additional Tables, Figures, Maps, and Related Publications*. Geological Survey of Finland, Espoo, pp. 519–540.

Liu, T.S., 1985. *Loess and the Environment*. China Ocean Press, Beijing, 251 pp.

Lukashev, K.I., Lukashev, V.K., Dobrovalskaya, I.A., 1965. Lithogeochemical properties of loess in Byelorussia and Central Asia. In: Schultz, C.B., Freye, C. (Eds.), *Proceedings of the 8th Congress, International Association for Quaternary Research, v. 12, Loess and Related Eolian Deposits of the World*. University of Nebraska Press, Lincoln, Nebraska.

Marković, S., Bokhorst, M., Vanderberghe, J., McCoy, W., Oches, E., Hambach, U., 2008. Late Pleistocene loess–paleosol sequences in the Vojvodina region, north Serbia. *Journal of Quaternary Science* **23**, 73–84.

Marković, S., Stevens, T., Kukla, G.J., Hambach, U., Fitzsimmons, K.E., Gibbard, P., Buggle, B., *et al.*, 2015. Danube loess stratigraphy – towards a pan-European loess stratigraphic model. *Quaternary Science Reviews* **148**, 228–258.

Maruszczak, H., 1991. Stratigraphical differentiation of Polish loesses. In: Maruszczak, H. (Ed.), *Main Sections of Loesses in Poland*. UMCS, Lublin, Poland, pp. 13–35. [in Polish, with English abstract]

McLennan, S.M., 1993. Weathering and global denudation. *Journal of Geology* **101**, 295–303.

McLennan, S.M., 2001. Relationships between the trace element composition of sedimentary rocks and upper continental crust. *Geochemistry, Geophysics, Geosystems* **2**, 1021. https://doi.org/10.1029/2000GC000109.

McLennan, S.M., Hemming, D.K., Hanson, G.N., 1993. Geochemical approaches to sedimentation, provenance and tectonics. In: Johnsson, M.A., Basu, A. (Eds.), Processes Controlling the Composition of Clastic Sediments. *Geological Society of America Special Papers* **284**, 21–40.

Miller, B.A., Schaetzl, R.J., 2012. Precision of soil particle size analysis using laser diffractometry. *Soil Science Society of America Journal* **76**, 1719–1727.

Miyazaki, T., Kimura, J.I., Katakuse, M., 2016. Geochemical records from loess deposits in Japan over the last 210 kyr: lithogenic source changes and paleoclimatic indications. *Geochemistry, Geophysics, Geosystems* **17**, 2745–2761.

Moska, P., Bluszcz, A., 2013. Luminescence dating of loess profiles in Poland. *Quaternary International* **296**, 51–60.

Moska, P., Adamiec, G., Jary, Z., Bluszcz, A., 2017. OSL chronostratigraphy for loess deposits from Tyszowce – Poland. *Geochronometria* **44**, 307–318.

Moska, P., Adamiec, G., Jary, Z., Bluszcz, A., Poręba, G., Piotrowska, N., Krawczyk, M., Skurzyński, J., 2018. Luminescence chronostratigraphy for the loess deposits in Złota, Poland. *Geochronometria* **45**, 44–55.

Moska, P., Jary, Z., Adamiec, G., Bluszcz, A., 2019a. Chronostratigraphy of a loess–palaeosol sequence in Biały Kościół, Poland using OSL and radiocarbon dating. *Quaternary International* **502**, 4–17.

Moska, P., Jary, Z., Adamiec, G., Bluszcz, A., 2019b. High resolution dating of loess profile from Strzyżów (Horodło Plateau–Ridge, Volhynia Upland). *Quaternary International* **502**, 18–29.

Mroczek, P., 2013. Recycled loesses – a micromorphological approach to the determination of local source areas of Weichselian loess. *Quaternary International* **296**, 241–250.

Muhs, D.R., 2018. The geochemistry of loess: Asian and North American deposits compared. *Journal of Asian Earth Sciences* **155**, 81–115.

Muhs, D.R., Bettis, E.A., 2000. Geochemical variations in Peoria loess of western Iowa indicate paleowinds of midcontinental North America during last glaciation. *Quaternary Research* **53**, 49–61.

Muhs, D.R., Budahn, J.R., 2006. Geochemical evidence for the origin of late Quaternary loess in central Alaska. *Canadian Journal of Earth Sciences* **43**, 323–337.

Nesbitt, H.W., 1979. Mobility and fractionation of rare earth elements during weathering of a granodiorite. *Nature* **279**, 206–210.

Nesbitt, H.W., Young, G.M., 1982. Early Proterozoic climate and plate motions inferred from major element chemistry of lutites. *Nature* **229**, 715–717.

https://doi.org/10.1017/qua.2023.69 Published online by Cambridge University Press

Nesbitt, H.W., Young, G.M., 1984. Prediction of some weathering trends of plutonic and volcanic rocks based on thermodynamic and kinetic considerations. *Geochimica et Cosmochimica Acta* **48**, 1523–1534.

Nesbitt, H.W., Young, G.M., McLennan, M., Keays, R.R., 1996. Effects of chemical weathering and sorting on the petrogenesis of siliciclastic sediments, with implications for provenance studies. *The Journal of Geology* **104**, 525–542.

Obreht, I., Zeeden, C., Schulte, P., Hambach, U., Eckmeier, E., Timar-Gabor, A., Lehmkuhl, F., 2015. Aeolian dynamics at the Orlovat loess–paleosol sequence, northern Serbia, based on detailed textural and geochemical evidence. *Aeolian Research* **18**, 69–81.

Pańczyk, M., Nawrocki, J., Bogucki, A.B., Gozhik, P., Łanczont, M., 2020. Possible sources and transport pathways of loess deposited in Poland and Ukraine from detrital zircon U–Pb age spectra. *Aeolian Research* **45**, 100598. https://doi.org/10.1016/j.aeolia.2020.100598.

Pötter, S., Seeger, K., Richter, C., Brill, D., Knaak, M., Lehmkuhl, F., Schulte, P., 2023. Pleniglacial dynamics in an oceanic central European loess landscape. *E&G Quaternary Science Journal* **72**, 77–94.

Pötter, S., Veres, D., Baykal, Y., Nett, J.J., Schulte, P., Hambach, U., Lehmkuhl, F., 2021. disentangling sedimentary pathways for the pleniglacial Lower Danube loess based on geochemical signatures. *Frontiers in Earth Science* **9**, 600010. https://doi.org/10.3389/feart.2021.600010.

Pye, K., 1984. Loess. *Progress in Physical Geography* **8**, 176–217.

Reeder, S., Taylor, H., Shaw, R.A., Demetriades, A., 2006. Introduction to the chemistry and geochemistry of the elements. In: Tarvainen, T., De Vos, W. (Eds.), *Geochemical Atlas of Europe. Part 2. Interpretation of Geochemical Maps, Additional Tables, Figures, Maps, and Related Publications*. Geological Survey of Finland, Espoo, pp. 48–429.

Rock, N.M.S., 1987. The need for standardization of normalised multi-elemental diagrams in geochemistry: a comment. *Geochemical Journal* **21**, 75–84.

Rollinson, H., 2013. *Using Geochemical Data: Evaluation, Presentation, Interpretation*. Routledge, Abingdon, UK.

Rousseau, D.-D., Chauvel, C., Sima, A., Hatte, C., Lagroix, F., Antoine, P., Balkanski, Y., *et al.*, 2014. European glacial dust deposits: geochemical constraints on atmospheric dust cycle modeling. *Geophysical Research Letters* **41**, 7666–7674.

Rousseau, D.-D., Derbyshire, E., Antoine, P., Hatté, C., 2018. *European Loess Records*. Reference Module in Earth Systems and Environmental Sciences, Elsevier, Amsterdam.

Rudnick, R.L., Gao, S., 2003. Composition of the continental crust. In: Holland, H.D., Turekian, K.K. (Eds.), *Treatise on Geochemistry,* vol. 3. Elsevier–Pergamon, Oxford–London, pp. 1–64.

Schaetzl, R.J., Attig, J.W., 2013. The loess cover of northeastern Wisconsin. *Quaternary Research* **79**, 199–214.

Schaetzl, R.J., Bettis III, A., Crouvi, O., Fitzsimmons, K.E., Grimley, D.A., Hambach, U., Lehmkuhl, F., *et al.*, 2018. Approaches and challenges to the study of loess – introduction to the LoessFest special issue. *Quaternary Research* **89**, 563–618.

Scheib, A.J., Birke, M., Dinelli, E., GEMAS Project Team, 2014. Geochemical evidence of aeolian deposits in European soils: geochemical evidence of aeolian deposits in European soils. *Boreas* **43**, 175–192.

Schnetger, B., 1992. Chemical composition of loess from a local and world-wide view. *Neues Jahrbuch fur Mineralogie Monatshefte* **1**, 29–47.

Shao, J., Yang, S., Li, C., 2012. Chemical indices (CIA and WIP) as proxies for integrated chemical weathering in China: inferences from analysis of fluvial sediments. *Sedimentary Geology* **265–266**, 110–120.

Sheldon, N.D., Tabor, N.J., 2009. Quantitative paleoenvironmental and paleoclimatic reconstruction using paleosols. *Earth-Science Reviews* **95**, 1–52.

Shepard, F.P., 1954. Nomenclature based on sand–silt–clay ratios. *Journal of Sedimentary Research* **24**, 151–158.

Shi, Y. E. C., Peng, Q., Zhang, Z., Zhang, J., Yan, W., Xu, C., 2023. Rare earth elements in aeolian loess sediments from Menyuan Basin, northeastern Tibetan plateau: implications for provenance. *Frontiers in Environmental Science* **11**, 1074909. https://doi.org/10.3389/fenvs.2023.1074909.

Sial, A.N., Gaucher, C., Ramkumar, M., Ferreira, V.P., 2019. Chemostratigraphy as a formal stratigraphic method. In: Sial, A.N., Gaucher, C., Ramkumar, M., Ferreira, V.P. (Eds.), Chemostratigraphy Across Major Chronological Boundaries. *Geophysical Monograph* **240**, 1–25.

Skurzyński, J., Fenn, K., 2022. Wpływ aspektów metodycznych na poprawność paleośrodowiskowych interpretacji zmienności cech geochemicznych w lessach. In: Łanczont, M., Hołub, M., Mroczek, P. (Eds.), *Metodyka rekonstrukcji zmian klimatu i środowiska zapisanych w pokrywach lessowych. XXI Terenowe Seminarium Korelacja lessów i osadów glacjalnych Polski i Ukrainy. Interdyscyplinarne Seminarium Naukowe Glacjał i peryglacjał Europy Środkowej*. Jarosław, 6–8 Października 2022 r., Lublin, Poland, pp. 77–82. [in Polish]

Skurzyński, J., Modelska, M., Raczyk, J., Staśko, S., Jary, Z., 2017. Skład chemiczny wód porowych górnoplejstoceńskiej sekwencji lessowo-glebowej w Zaprężynie (SW Polska). *Przegląd Geologiczny* **65**, 1383–1387. [in Polish, with English abstract]

Skurzyński, J., Jary, Z., Raczyk, J., Moska, P., Korabiewski, B., Ryzner, K., Krawczyk, M., 2019. Geochemical characterization of the Late Pleistocene loess–palaeosol sequence in Tyszowce (Sokal Plateau–Ridge, SE Poland). *Quaternary International* **502**, 108–118.

Skurzyński, J., Jary, Z., Kenis, P., Kubik, R., Moska, P., Raczyk, J., Seul, C., 2020. Geochemistry and mineralogy of the Late Pleistocene loess–palaeosol sequence in Złota (near Sandomierz, Poland): implications for weathering, sedimentary recycling and provenance. *Geoderma* **375**, 114459. https://doi.org/10.1016/j.geoderma.2020.114459.

Smalley, I.J., Leach, J.A., 1978. The origin and distribution of the loess in the Danube basin and associated regions of East-Central Europe: a review. *Sedimentary Geology* **21**, 1–26.

Smalley, I., Vita-Finzi, C., 1968. The formation of fine particles in sandy deserts and the nature of "desert" loess. *Journal of Sedimentary Research* **38**, 766–774.

Smalley, I.J., O'Hara-Dhand, K., Wint, J., Machalett, B., Jary, Z., Jefferson, I.F., 2009. Rivers and loess: the significance of long river transportation in the complex event-sequence approach to loess deposit formation. *Quaternary International* **198**, 7–18.

Song, Y., Chen, X., Qian, L., Li, C., Li, Y., Li, X., 2014. Distribution and composition of loess sediments in the Ili Basin, Central Asia. *Quaternary International* **334–335**, 61–73.

Stevens, T., Adamiec, G., Bird, A.F., Lu, H., 2013. An abrupt shift in dust source on the Chinese Loess Plateau revealed through high sampling resolution OSL dating. *Quaternary Science Reviews* **82**, 121–132.

Svensson, D.N., Messing, I., Barron, J., 2022. An investigation in laser diffraction soil particle size distribution analysis to obtain compatible results with sieve and pipette method. *Soil and Tillage Research* **223**, 105450. https://doi.org/10.1016/j.still.2022.105450.

Taylor, S.R., McLennan, S.M., 1985. *The Continental Crust: Its Composition and Evolution*. Blackwell, London.

Taylor, S.R., McLennan, S.M., McCulloch, M.T., 1983. Geochemistry of loess, continental crustal composition and crustal model ages. *Geochimica et Cosmochimica Acta* **47**, 1897–1905.

Templ, M., Filzmoser, P., Reimann, C., 2008. Cluster analysis applied to regional geochemical data: problems and possibilities. *Applied Geochemistry* **23**, 2198–2213.

Tripathi, J.K., Rajamani, V., 1999. Geochemistry of the loessic sediments on Delhi ridge, eastern Thar Desert, Rajasthan: implications for exogenic processes. *Chemical Geology* **155**, 265–278.

Tu, X.B., Kwong, A.K.L., Dai, F.C., Tham, L.G., Min, H., 2009. Field monitoring of rainfall infiltration in a loess slope and analysis of failure mechanism of rainfall-induced landslides. *Engineering Geology* **105**, 134–150.

Tutkovsky, P.A., 1899. K voprosu o sposobe obrazovaniya lessa. *Zemlevedenie* **1–2**, 213–311. [in Russian]

Újvári, G., Varga, A., Balogh-Brunstad, Z., 2008. Origin, weathering, and geochemical composition of loess in southwestern Hungary. *Quaternary Research* **69**, 421–437.

Újvári, G., Varga, A., Raucsik, B., Kovacs, J., 2014. The Paks loess–paleosol sequence: a record of chemical weathering and provenance for the last 800 ka in the mid-Carpathian Basin. *Quaternary International* **319**, 22–37.

https://doi.org/10.1017/qua.2023.69 Published online by Cambridge University Press

Van Loon, A.J., 2006. Lost loesses. *Earth-Science Reviews* **74**, 309–316.

Varga, A., Újvári, G., Raucsik, B., 2011. Tectonic versus climatic control on the evolution of a loess-paleosol sequence at Beremend, Hungary: an integrated approach based on paleoecological, clay mineralogical, and geochemical data. *Quaternary International* **240**, 71–86.

Waroszewski, J., Pietranik, A., Sprafke, T., Kabała, C., Frechen, M., Jary, Z., Kot, A., *et al.*, 2021. Provenance and paleoenvironmental context of the late Pleistocene thin aeolian silt mantles in southwestern Poland – a widespread parent material for soils. *Catena* **204**, 105377. https://doi.org/10.1016/j.catena.2021.105377.

Wentworth, C.K., 1922. A scale of grade and class terms for clastic-sediments. *The Journal of Geology* **30**, 377–392.

Wilson, M.J., 2004. Weathering of the primary rock-forming minerals: processes, products and rates. *Clay Minerals* **39**, 233–266.

Wright, J.S., Smith, B., Whalley, B., 1998. Mechanisms of loess-sized quartz silt production and their relative effectiveness: laboratory simulations. *Geomorphology* **23**, 15–34.

Yang, S., Ding, F., Ding, Z., 2006. Pleistocene chemical weathering history of Asian arid and semi-arid regions recorded in loess deposits of China and Tajikistan. *Geochimica et Cosmochimica Acta* **70**, 1695–1709.

Zeng, R.Q., Meng, X.M., Zhang, F.Y., Wang, S.Y., Cui, Z.J., Zhang, M.S., Zhang, Y., Chen, G., 2016. Characterizing hydrological processes on loess slopes using electrical resistivity tomography – a case study of the Heifangtai Terrace, Northwest China. *Journal of Hydrology* **541**,742–753.

Zöller, L., Fischer, M., Jary, Z., Antoine, P., Krawczyk, M., 2022. Chronostratigraphic and geomorphologic challenges of last glacial loess in Poland in the light of new luminescence ages. *E&G Quaternary Science Journal* **71**, 59–81.

https://doi.org/10.1017/qua.2023.69 Published online by Cambridge University Press